Lithos 120 (2010) 96–115

Contents lists available at ScienceDirect

Lithos

journal homepage: www.elsevier.com/locate/lithos

Concordant structural variations from the surface to the base of the upper mantle in the North China Craton and its tectonic implications

Ling Chen *

Seismological Laboratory (SKL-LE), Institute of Geology and Geophysics, Chinese Academy of Sciences, Beijing 100029, China

ARTICLE INFO

Article history:
Received 7 May 2009
Accepted 14 December 2009
Available online 29 December 2009

Keywords:
North China Craton
Lithospheric reactivation
Concordant structural variation
Pre-existing structure
Pacific subduction

ABSTRACT

This study presents an integrated study of the North China Craton (NCC) based on recent high-resolution seismic images combined with observations on surface geology, regional tectonics and mantle dynamics. Seismic images reveal markedly concordant and rapid variations in crustal and lithospheric structure and thickness, upper mantle anisotropy, and discontinuity structures and thickness of the mantle transition zone near the boundary between the eastern and central parts of the NCC. These rapid variations roughly coincide with the sudden change in both surface topography and gravity field as marked by the North–South Gravity Lineament (NSGL). Such a shallow–deep structural concordance may reflect different lithospheric tectonics and mantle processes in the two domains during the Phanerozoic reactivation of the craton. Sharp structural variations are particularly present to the west of the NSGL, especially between the Archean Ordos Plateau, which retains the characteristics of a typical craton, and the surrounding Cenozoic rift systems which are underlain by a significantly modified and thinned lithosphere. These observations provide deep structural evidence that the Phanerozoic reactivation was not confined to the eastern NCC as previously thought, but also affected areas in the central and western NCC, though to a much lesser degree. On both sides of the NSGL, lithospheric modification and thinning appear to be more pronounced along Paleoproterozoic belts suturing Archean blocks, demonstrating the importance of pre-existing lithosphere-scale structures in controlling the tectonic evolution of the NCC. It further indicates that craton reactivation probably is common given the fact that structural heterogeneities are always present in cratonic regions. The seismic structural images together with geological, petrological, geochemical and mineral physics data suggest that the fundamental destruction of the eastern NCC lithosphere may have been triggered largely by the deep subduction of the Pacific plate, especially during the Late Mesozoic. The complexity of deep structures and lithospheric properties in regions west of the NSGL may represent the relatively weak imprints of the Cenozoic India–Eurasia collision superposed upon that of the earlier tectonic events.

1. Introduction

Detailed studies of the structures at different depths under the Earth's continent and their variable response to plate tectonics can provide crucial information for a better understanding of the evolution of continental lithosphere, particularly the stabilization/destabilization of cratons over a long span of geological time. The North China Craton (NCC), located on the eastern margin of Asia (Fig. 1a), contains crustal rocks as old as 3.8 Ga (Liu et al., 1992), and is an ideal place for such studies because Phanerozoic tectonic activity has led to fundamental reactivation and destruction of the cratonic lithosphere and marked structural heterogeneities in this region.

The NCC is composed of two major Archean blocks, the eastern and western NCC, separated by a Paleoproterozoic orogen known as the Trans-North China Orogen (central NCC) (Zhao et al., 2001, 2005; Fig. 1b). The craton as a whole had characteristics similar to those of other cratons before the Middle Ordovician (e.g., Menzies et al., 1993; Griffin et al., 1998; Gao et al., 2002), having been stable for at least 1500 Ma ever since its final cratonization ~1.85 Ga ago (Zhao et al., 2001, 2005). However, the craton exhibits two distinct geologic features at the present time, possibly the surface expressions of later tectonic diversity between the different constituent parts of the craton (Xu et al., 2004a; Xu, 2007). One is the marked variation in surface topography, with lowlands mostly less than 200 m in altitude in the east, and mountains or plateaus higher than 1200–1500 m (up to 3500 m) in the west (Figs. 1 and 2). This sharp topographic change roughly coincides with the NEE-trending North–South Gravity Lineament (NSGL, thick gray line in Figs. 1 and 2) which separates significantly negative gravity anomalies (<−100 mGal) to the west and weakly negative to positive anomalies (>−20 mGal) to the east (Ma, 1989). Both changes occur in large part close to the boundary between the eastern and central NCC (Fig. 2), and extend outside of the NCC both to the north and south, affecting the entire eastern

* Tel.: +86 10 82998416; fax: +86 10 62010846.
E-mail address: lchen@mail.iggcas.ac.cn.

0024-4937/$ – see front matter © 2009 Elsevier B.V. All rights reserved.
doi:10.1016/j.lithos.2009.12.007

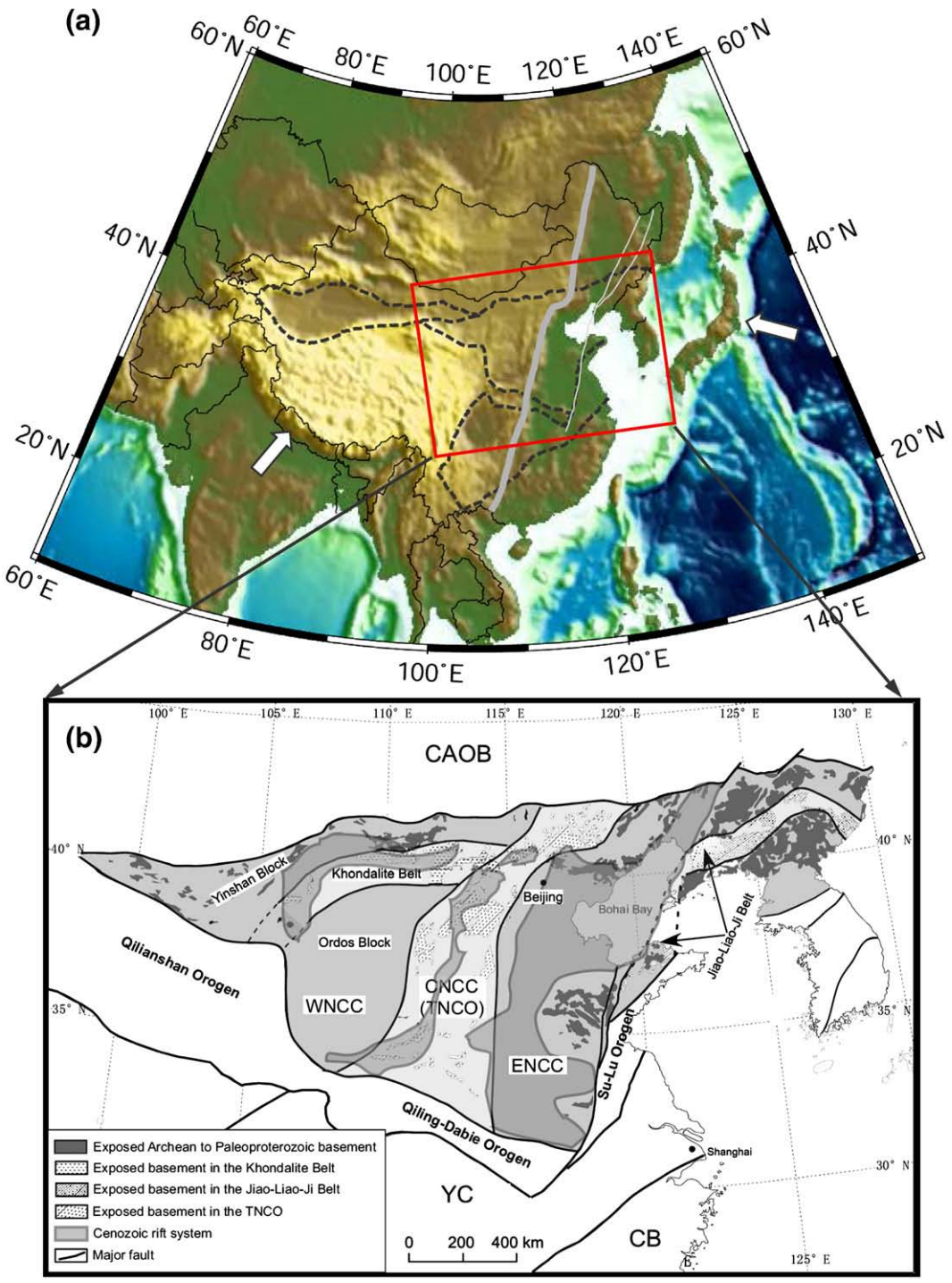

Fig. 1. (a) Map of China and neighboring regions. Dashed lines outline the North China Craton (NCC), Yangtze Craton and Tarim Craton. Thick gray line marks the North–South Gravity Lineament (NSGL) which separates two topographically different domains. Thin gray lines represent the Tanlu Fault Zone near the eastern margin of China. White arrows show the subduction direction of the Pacific plate in the east and the indentation direction of the Indian plate in the southwest; (b) geological map (modified from Zhao et al., 2005) showing exposed basement and Cenozoic rift systems of the NCC. ENCC, CNCC (TNCO) and WNCC denote three-fold subdivision of the craton into the eastern and western parts, with the Trans-North China Orogen between them. YC — Yangtze Craton, CB — Cathaysia Block, CAOB — Central Asia Orogenic Belt.

China continent (Fig. 1a). The present-day distinct changes in topography and gravity field suggest that the opposite sides of the NSGL may have evolved differently in the Phanerozoic.

The eastern NCC has undergone significant tectonothermal reactivation and destruction with a dramatic change in lithospheric architecture during the period from the Ordovician to the Cenozoic. This is evidenced by basalt-borne xenoliths and geophysical observations that reveal that a thin (<100 km), hot (~65 mW/m^2) and fertile lithosphere has been widespread beneath this region from the early Cenozoic to the present time (e.g., Chen et al., 1991; Menzies et al., 1993; Griffin et al., 1998; Fan et al., 2000; Xu, 2001; Zhu et al., 2002; Huang et al., 2003; Wu et al., 2005; Chen et al., 2006a, 2008), in striking contrast to the thick (>180 km), cold (~40 mW/m^2) and refractory Paleozoic lithosphere sampled by xenolith-bearing diamondiferous kimberlites (Menzies et al., 1993; Griffin et al., 1998; Gao et al., 2002).

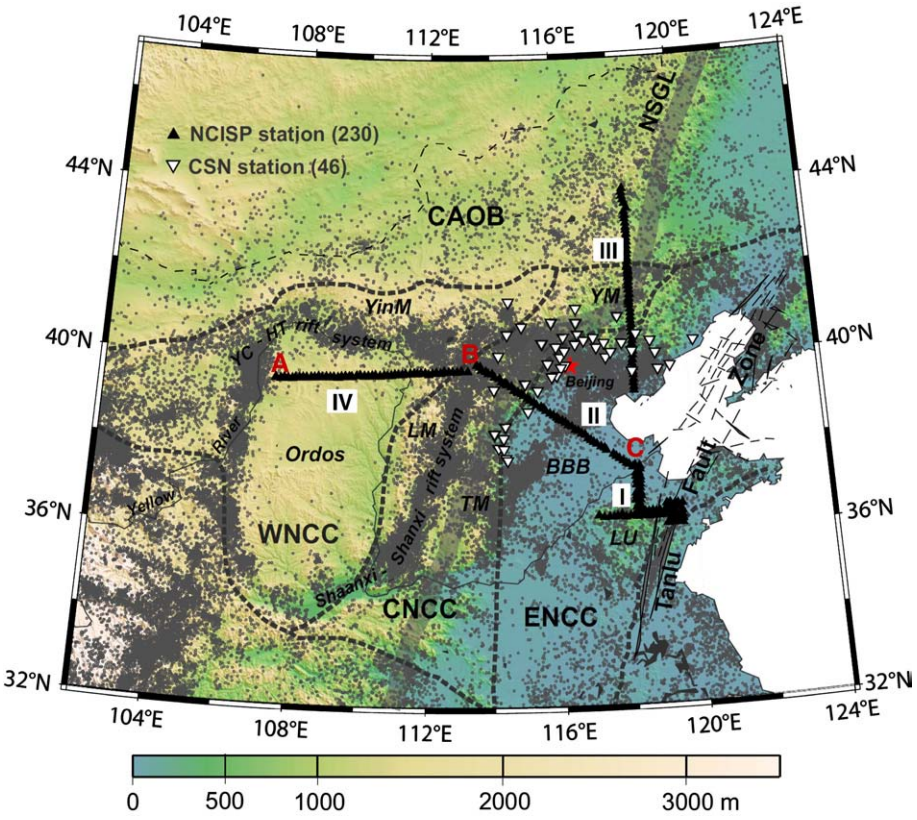

Fig. 2. Surface topography, seismicity (1960–2004, gray circles) and major tectonic units of the study region, including the Tanlu Fault Zone, Luxi Uplift (LU), Bohai Bay Basin (BBB), Taihang Mountains (TM), Lüliang Mountains (LM), Yan Mountains (YM), Yin Mountains (YinM), Ordos Plateau, Yinchuan–Hetao (YC–HT) and Shaanxi–Shanxi rift systems. Broadband seismic stations are also shown, including 230 stations which form four sub-arrays (I–IV) under the North China Interior Structure Project (NCISP) (black triangles) and 46 stations belonging to the Capital Seismic Network (CSN) (inverted triangles). A, B, and C mark the starting and ending locations of the NCISP-II and IV arrays used for the integrated crustal shear velocity model (Zheng et al., 2009) shown in Fig. 6a.

It has been proposed that most of the central and western NCC have remained stable since the Precambrian (e.g., Zhai and Liu, 2003; Kusky et al., 2007), based primarily on geological mapping and large-scale geophysical surveys that show rare magmatic activity, relatively low heat flow (Wang et al., 1996; Hu et al., 2000) and generally thick crust (Ma, 1989; Li et al., 2006) and lithosphere (Chen et al., 1991; Zhu et al., 2002) in these regions. However, recent detailed petrological and geochemical studies of Cenozoic basalts and their entrained peridotite xenoliths as well as Mesozoic mafic intrusions suggest that lithospheric modification and thinning may also have taken place locally near the rifted or marginal areas in the central NCC (e.g., Xu et al., 2004a; Tang et al., 2006; Wang et al., 2006; Xu, 2007). Localized lithospheric thinning in the central and even western NCC is also implied by available high-resolution seismic images from dense-array data (e.g., Huang et al., 2009; Chen, 2009; Chen et al., 2009) and magnetotelluric observations (Wei et al., 2008). These results demonstrate a high degree of lithospheric heterogeneity with the coexistence of both significantly thinned and preserved thick mantle roots under regions west of the NSGL, in contrast to the widespread thinned lithosphere to the east. Combined with the sharp changes in surface topography and gravity (Figs. 1a and 2), these observations corroborate the previous idea that the central and western parts of the craton have evolved in a fundamentally different regime from their eastern counterpart during Phanerozoic time (Xu et al., 2004a; Xu, 2007).

The mechanism and dynamic trigger of the Phanerozoic lithospheric reactivation of the NCC and the causes of the different behaviors of the three parts of the NCC during the reactivation process are currently still controversial. Several tectonic factors including the deep subduction of Palaeo-Pacific plate (Griffin et al., 1998; Wu et al., 2003a; Sun et al., 2007), collision of an amalgamated North China–Mongolian plate with the Siberian plate (Davis et al., 2001), enhanced mantle temperature associated with plumes (Deng et al., 2004), the India–Eurasia collision (Menzies et al., 1993) and the North China–South China collision (Yin and Nie, 1996; Zhang, 2007) have been proposed as explanations. These hypotheses were based on specific studies mostly confined to the eastern NCC and boundary regions, and appear to be incapable of reconciling all types of observations (e.g., Wu et al., 2008 and references therein). How the various tectonic events affected the central and western NCC is much less known, due largely to the paucity of data. A better understanding of the Phanerozoic lithospheric tectonics and deep dynamics of the entire NCC demands further evidence, especially detailed knowledge of the structures and properties of the crust, lithosphere and deep upper mantle under the NCC and the relationship between the structural variations at different depth levels and in different parts of the craton.

To achieve this goal, a seismic experiment named the Northern China Interior Structure Project (NCISP) has been carried out since 2000 by the Institute of Geology and Geophysics, Chinese Academy of Sciences. Under this project more than 200 temporary broadband seismic stations have been deployed in the NCC with average inter-station spacing of about 10 km (black triangles in Fig. 2). These stations formed four linear arrays (I to IV, four sub-projects of the NCISP), traversing the major tectonic units and boundary zones of the region (Fig. 2). In addition to the NCISP temporary arrays, a number of stations from the permanent broadband seismic networks belonging to the China Earthquake Administration (CEA) have also been used (shown as inverted triangles in Fig. 2). For more detailed information about the stations and the data, refer to our previous publications (e.g., Zheng et al., 2006; Zhao et al., 2008; Chen et al., 2008, 2009) or

visit the website http://www.seislab.cn/data/ for NCISP seismic arrays. Based on these data, a number of studies have revealed distinct features and substantial heterogeneities in crustal structure (e.g., Zheng et al., 2006, 2007, 2008a,b, 2009), lithospheric thickness and the structure of the lithosphere-asthenosphere boundary (LAB) (e.g., Chen et al., 2006a, 2008; Tang and Chen, 2008; Chen et al., 2009), upper mantle anisotropy (e.g., Zhao and Zheng, 2005, 2007; Zhao et al., 2007b, 2008), and mantle transition zone structure (e.g., Ai and Zheng, 2003; Chen et al., 2006b; Chen and Ai, 2009) under the NCC.

In this study, I integrate our previous work on the NCC and systematically compare the structural variations at different depth levels and between different constituent parts of the craton. From a regional point of view and combining other geophysical observations as well as geological, petrographic and geochemical data, I especially focus on the structural changes across the NSGL and within the central and western NCC, and their correlations with surface tectonics and mantle dynamics. On the basis of these comparisons, I discuss the possible tectonic causes for the lithospheric reactivation and destruction of the NCC and present a tectonic model of the Phanerozoic evolution of the NCC.

2. Geological setting

The NCC formed in Paleoproterozoic time by the assembly of the eastern and western NCC along the Trans-North China Orogen (Zhao et al., 2001, 2005). The craton consists of variably exposed Early Archean to Paleoproterozoic basement overlain by Mesoproterozoic to Cenozoic cover. The Paleoproterozoic basement rocks are not distributed randomly in the eastern and western NCC, but are exposed along linear structural belts (Fig. 1b, Zhao et al., 2005). In the eastern NCC, the Paleoproterozoic rocks are mainly exposed along the NE-trending Jiao-Liao-Ji Belt which probably developed after the final closure of the Paleoproterozoic rift system in this region at ~1.9 Ga. In the western NCC Paleoproterozoic rocks crop out along the nearly EW-trending Khondalite Belt, which represents a continental collision belt along which the Yinshan (Yin Mountain) Block in the north and the Ordos Block in the south collided to form the Western NCC some time before the amalgamation of the western and eastern NCC (Zhao et al., 2003).

Morphologically, the NCC is bounded to the west by the early Paleozoic Qilianshan Orogen, to the north by the late Paleozoic Central Asia Orogenic Belt, and to the south and east by the Mesozoic Qinling-Dabie-Su-Lu Orogen (Fig. 1b). The Qilianshan Orogen was created by multiple subduction–accretion events from the Cambrian to the Devonian before final amalgamation and docking with the westernmost part of the NCC (e.g., Xiao et al., 2002; Pan et al., 2006; Xiao et al., 2009). The generally EW-trending Central Asia Orogenic Belt formed through NS-directed subduction of the Paleo-Asian ocean and subsequent arc–arc, arc–continent, and continent–continent collision mainly during the Paleozoic, leading to the final amalgamation of the

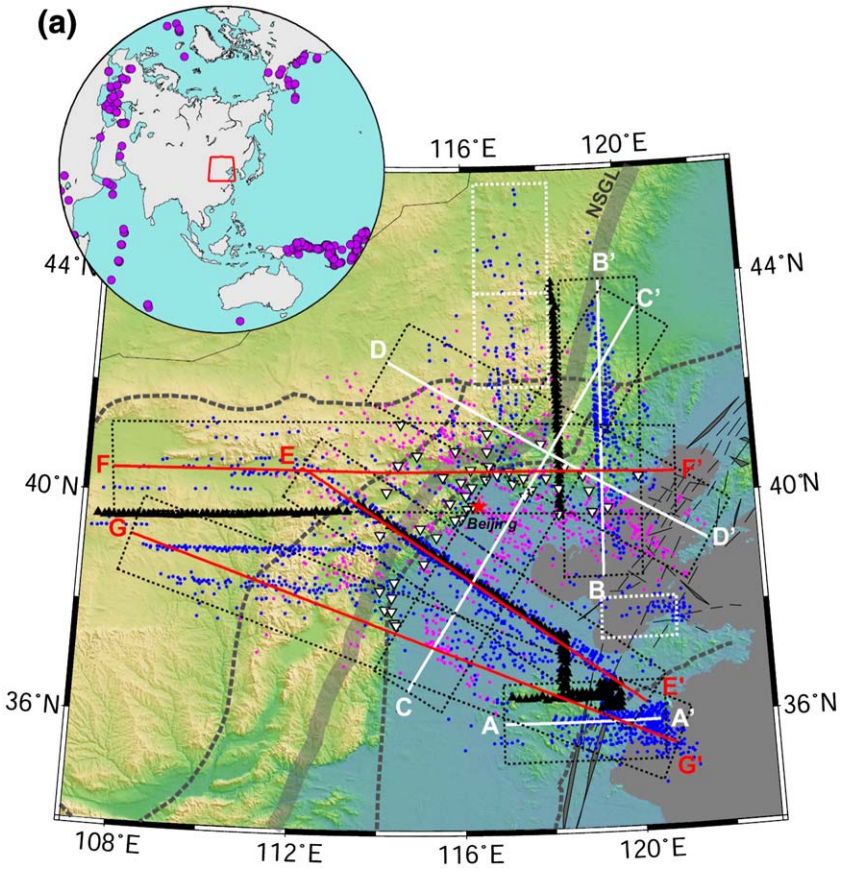

Fig. 3. (a) S-RF data coverage, individual stacking blocks (white rectangles) where the S-RFs are insufficient for migration and imaging profiles (solid lines) for which S-RF migrations were conducted previously to construct the lithospheric images: profiles A–A′to D–D′, Chen et al. (2008); E–E′, Chen (2009); and F–F′ and G–G′, Chen et al. (2009). Piercing points at 100-km depth for S-to-P converted phases are shown as blue dots (for NCISP stations) and purple dots (for CEA stations). Black rectangle around each profile marks the area where the S-RFs are projected onto the profile for imaging. Map inset shows the distribution of teleseismic events used. (b) Surface topography, Bouguer gravity anomaly, and migrated S-RF images for the three profiles E–E′ to G–G′ (red lines in a) which traverse all three constituent parts of the NCC. Red and blue colors represent positive and negative amplitudes, respectively. Black dashed lines denote the LAB estimated from the corresponding S-RF images. For profile G–G′, both higher-frequency (0.03–0.35 Hz) and lower-frequency (0.03–0.18 Hz) images are shown to illustrate the consistency of the LAB image. White dashed lines mark the Moho imaged either from the S-RFs (profile G–G′) or from the P-RFs if available (profiles E–E′ and F–F′, Zheng et al., 2006; Chen, 2009; Chen et al., 2009). Black arrows mark rapid changes in the LAB depth. Labels for the major tectonic units as in Figs. 1b and 2 except that the Shaanxi–Shanxi rift system is denoted as S–S RS.

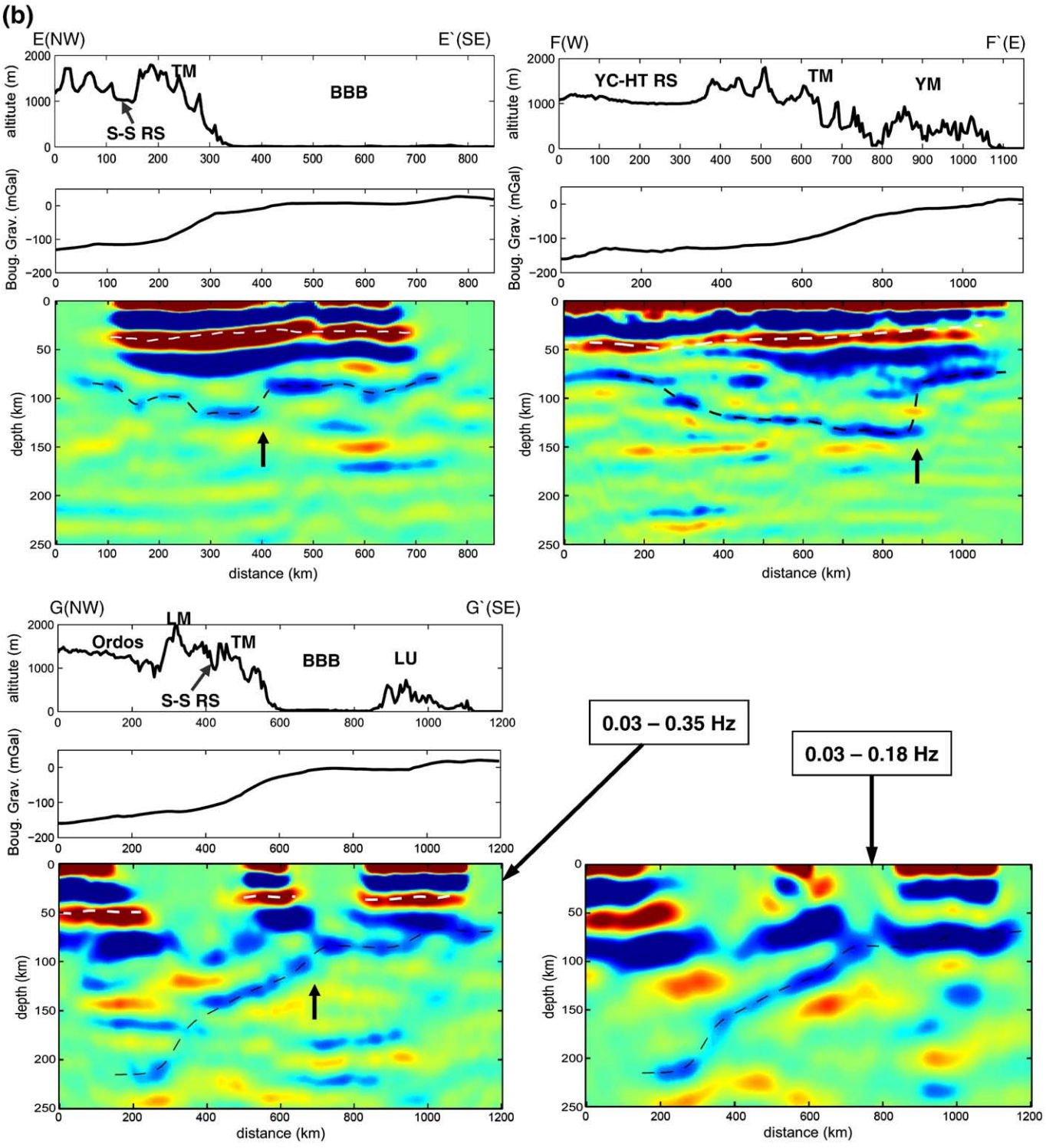

Fig. 3 (*continued*).

NCC to the Siberian craton (Sengör et al., 1993; Davis et al., 2001; Xiao et al., 2003). The Mesozoic N–S intraplate shortening and uplift of the Yin-Yan Mountains in the northern boundary region of the NCC (Fig. 2) may be a consequence of this collision and postcollisional tectonics (Davis et al., 2001). The Qinling-Dabie-Su-Lu Orogen has formed as a result of the Triassic collision and subduction of the Yangtze Craton beneath the NCC (Li et al., 1993). This continental collision event was also responsible for the development of the Tanlu Fault Zone, a major strike-slip fault zone extending for thousands of kilometers along the eastern margin of the eastern NCC (Yin and Nie, 1993; Zhang, 1997; Faure et al., 2001). The Tanlu Fault Zone is proposed to have facilitated the Mesozoic–Cenozoic asthenospheric upwelling and lithospheric reactivation of the eastern NCC (Zheng et al., 1998; Xu, 2001; Xu et al., 2004b; Chen et al., 2006a; Zheng et al., 2008b).

In the middle Mesozoic, oceanic plates including the Izanagi, Kula and Pacific plates began to subduct successively underneath the eastern margin of Asia (Maruyama et al., 1997; Bartolini and Larson,

2001; Smith, 2007). Subsequently, the geodynamic framework of the NCC changed from an E–W compressive tectonic regime to an extensional regime with a dominant NE–SW tectonic trend (Ren, 1990; Liu et al., 1997; Zhai et al., 2004). Since then the NCC has been the site of intensive lithospheric extension, resulting in the development of two different extensional domains on the two sides of the NSGL (Ye et al., 1987; Zhang et al., 2003).

The eastern extensional domain involves a large part of the eastern NCC (Fig. 1b), corresponding to the North China rift system that comprises the Bohai Bay basin in the north and the Southern North China Basin in the south. Extension of this domain started in the Late Jurassic–Early Cretaceous, and became widespread in Paleocene to Eocene time (Liu, 1987; Ma and Wu, 1987; Ye et al., 1987), accompanied by voluminous magmatism (Ren et al., 2002). Tectonically coupled with the formation of the North China rift system, the Taihang Mountains, which roughly coincide with the NSGL (Fig. 2), developed to the west (Liu et al., 2000).

Widespread lithospheric extension was absent in the western domain. Extensional deformation is localized in two elongate Cenozoic rift systems surrounding the Ordos Plateau: the S-shaped Shaanxi–Shanxi rift to the east and southeast, and the arc-shaped Yinchuan–Hetao rift to the northwest (Zhang et al., 1998, 2003, Fig. 1b). Extension in these zones began during the Eocene but was less active and did not extend to the whole periphery of the Ordos block until the Pliocene. Besides the subsidence history, geological and geophysical data have also revealed big differences in structural style and neotectonics between the rift systems on the eastern and western sides of the NSGL (e.g., Ye et al., 1987; Ma, 1989; Zhang et al., 1998, 2003).

In contrast to the eastern NCC and the circum-Ordos rift systems, the interior of the western NCC, i.e. the Ordos Plateau, appears to have retained the characteristics of a stable craton, as evidenced by a low heat flow (Wang et al., 1996; Hu et al., 2000), an absence of earthquakes (Fig. 2), and an apparent lack of internal deformation since the Precambrian (Zhai and Liu, 2003; Kusky et al., 2007).

3. Lithospheric structural imaging and LAB depth

The present-day lithospheric structure of the NCC may provide direct clues to the geographic scope and spatial variations of the Phanerozoic remobilization and thinning of the cratonic lithosphere, and therefore is of key importance for understanding the destruction of the craton. We have recently constructed lithospheric structural images along different linear profiles in the NCC (Fig. 3a) by wave equation-based migration of S-receiver functions (S-RFs) from more than 250 broadband seismic stations of the NCISP arrays and the CEA network (Fig. 3a; Chen et al., 2008, 2009; Chen, 2009). The S-RFs contain information on S-to-P (Sp) conversions from deep velocity discontinuities, which can be used to constrain the depths of the corresponding discontinuities (Farra and Vinnik, 2000). The S-to-P conversion from the Moho appears to be the strongest signal in the individual S-RFs, and hence can be easily identified in the migrated S-RF images (red signals marked by white dashed lines in Fig. 3b). In addition, the LAB can be detected continuously along all the profiles (blue signals marked by black dashed lines in Fig. 3b). The structural feature of the LAB was verified by the consistency of migrated images with different frequency contents of the S-RFs (e.g., Fig. 3b for profiles G–G′), by agreement between the S- and the P-RF images for the same areas, and agreement between the data images and synthetic testing results based on the actual data coverage (Chen et al., 2008, 2009; Chen, 2009). The RF images also agree broadly with both surface wave (Tang and Chen, 2008; Huang et al., 2009) and body wave (Huang and Zhao, 2006; Xu and Zhao, 2009) tomography results of the region, which further confirms the robustness of the imaged structure. Overall, our migrated images show significant topography on both the Moho (~30–50 km) and the LAB (~80–~210 km), suggesting substantial structural heterogeneity in the lithosphere beneath the NCC.

To gain a general picture of the regional lithospheric thickness, I have integrated the results of our S-RF migration for individual profiles (Chen et al., 2008, 2009; Chen, 2009) and stacking for individual blocks (white rectangles in Fig. 3a, Chen et al., 2008) to produce a map of the LAB depth across the study region (Fig. 4). By incorporating the data from the dense NCISP-IV and NCISP-II seismic arrays (Fig. 2), it is possible to expand our previous LAB depth map for the northeastern NCC (Fig. 9 in Chen et al., 2008) to cover regions further west including the northern part of the western and central NCC (Fig. 4). This allows comparison of the lithospheric thickness among the three parts of the craton.

The most striking feature of the new LAB depth map is perhaps the highly variable lithospheric thickness, which ranges from around 80 km to more than 200 km in the central and western NCC, in marked contrast to the widespread thinned lithosphere of 60–100 km in the eastern NCC (Fig. 4). This picture is at odds with a number of previous seismic studies (e.g., Chen et al., 1991; Zhu et al., 2002) that demonstrated only a thicker lithosphere in the central and western NCC compared to their eastern counterpart, and argued against notable lithospheric thinning in the central and western regions. However, the imaging results presented in those studies were obtained from much sparser data sets and using methods that have relatively poor spatial resolution compared to the S-RF imaging used here to study the LAB structure. Based on data from dense seismic arrays, our migrated S-RF images suggest substantial structural heterogeneity, and in particular the coexistence of both dramatically thinned and preserved thicker lithosphere in the central and western NCC (Fig. 4).

In addition to the significant lateral variations in lithospheric thickness, our S-RF and in some cases also P-RF data reveal a relatively sharp lithosphere–asthenosphere transition, with an S-wave velocity drop of several percent over a depth interval of ~5–20 km, in the eastern and northern parts of the NCC where the lithosphere has been notably thinned (Chen et al., 2006a, 2008). The pronounced and sharp LAB cannot be defined solely by temperature, but suggests the presence of volatiles or melt in the asthenosphere (Karato and Jung, 1998; Rychert et al., 2005; Chen et al., 2006a), which agrees with recent tomographic results that show a distinct low-velocity zone (LVZ) beneath the region (Huang and Zhao, 2006; Huang et al., 2009; Xu and Zhao, 2009). This type of LAB is analogous to what has been observed beneath oceanic and off-craton areas (e.g., Gaherty et al., 1999; Tan and Helmberger, 2007; Schutt et al., 2008) but different from that of most stable continental regions where the LVZ is either absent or much weak (e.g., Freybourger et al., 2001; Bruneton et al., 2004; Larson et al., 2006). The LAB images from our S- and P-RF studies therefore suggest that the Phanerozoic lithospheric reactivation of the NCC may not be a purely mechanical thinning process, but probably involved complex modification of the physical and chemical properties of the lithosphere. This is consistent with petrologic and geochemical observations on the mantle xenoliths of the region (e.g., Menzies et al., 1993; Griffin et al., 1998; Fan et al., 2000; Xu, 2001) that indicate a change in the nature of the lithosphere from cratonic to more fertile during the Phanerozoic. However, because of the relatively scattered sampling and limited coverage of the data (Fig. 3a), the sharpness of the LAB beneath the thick lithosphere areas especially in the western NCC has not yet been well constrained.

4. Lithospheric thickness *vs* surface geology, crustal structure and upper mantle anisotropy

To better understand the geological and tectonic background of the lithospheric thickness variations in the NCC, in this Section 1 compare in detail the estimated LAB depths with the altitude, surface tectonics, Bouguer gravity field, shear velocity structure of the crust, and seismic anisotropy of the upper mantle along both individual profiles (Figs. 3b, 5 and 6) and from a wider regional point of view

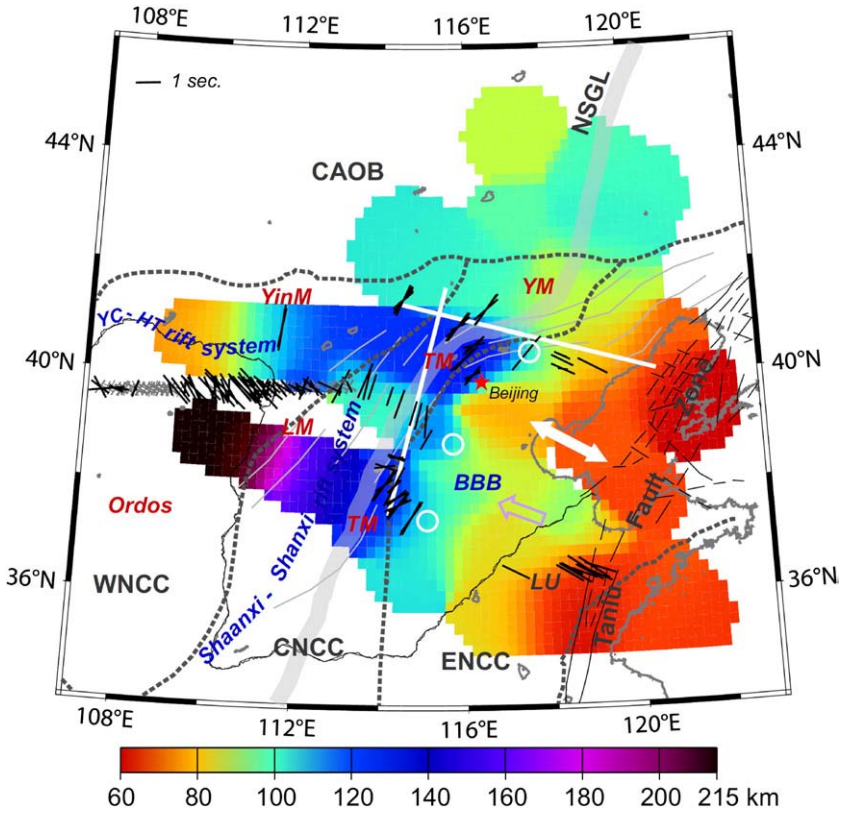

Fig. 4. Map of LAB depth for the study region. A Gaussian cap with a radius of 50 km and a maximum effective radius of 120 km was used in the depth interpolation. Short black bars and gray cross-bars show the SKS splitting measurements (Zhao and Zheng, 2005; Zhao et al., 2008). The orientation and length of each black bar represent the fast polarization direction and splitting delay time, respectively. Gray cross-bar indicates a null measurement, with orientation parallel or perpendicular to the polarization direction of the incoming energy. White circles mark the locations where rapid changes in the LAB depth are observed (as indicated by black arrows in Fig. 3b). Thin gray lines schematically indicate the trends of the Taihang Mountains and the Yan Mountains (Zhang, 1997). Single- and double-headed arrows give the average direction of absolute plate motion from HS3-NUVEL1A (Gripp and Gordon, 2002) and the possible extension direction of the eastern NCC during the Late Mesozoic to Early Cenozoic, respectively. The profile considered in Fig. 5 is shown as thick white line. Labels for the major tectonic units are same as Figs. 1b and 2.

(Fig. 4). The crustal shear velocity models were constructed by Zheng et al. (2006, 2008a, 2009) based on waveform inversion of stacked P-receiver functions (P-RFs, similar to S-RFs but using P-to-S conversions from subsurface discontinuities) for individual stations, and the upper mantle seismic anisotropy was measured by Zhao et al. through SKS splitting analysis (Zhao and Zheng, 2005; Zhao et al., 2008).

4.1. Lithospheric thickness vs surface geology

As we have already reported, the lithospheric thickness of the NCC appears to correlate well with the surface topography, tectonic divisions and gravity field of the region (Chen et al., 2008, 2009; Chen, 2009). This can be seen more explicitly by comparing the LAB depth with altitude and the Bouguer anomaly along each of the imaging profiles that traverse different parts of the craton (Fig. 3b), and is also obvious in the integrated LAB depth map (Fig. 4).

Four prominent features are present both along the image profiles and in the regional map. The first-order feature is the striking difference in the gravity field across the NSGL, where a rapid drop of more than 100 mGal in Bouguer gravity anomaly takes place within ~200 km laterally (middle panel for each profile in Fig. 3b). Widespread thinned lithosphere appears in the east and generally thick lithosphere in the west, with a rapid thickening of the lithosphere on the order of 20–40 km occurring over a lateral distance of ~100 km between the two blocks (black arrows in Fig. 3b and white circles in Fig. 4). The rapid thickening of the lithosphere begins about 50–100 km east of the sudden change in surface topography (Fig. 3b) and 100–200 km east of the obvious drop in the Bouguer gravity anomaly (Figs. 3b and 4). This discrepancy between the location of the change in lithospheric thickness and the NSGL cannot be attributed to the limited lateral resolution of the S-RF data (~100 km, Chen et al., 2008; Chen, 2009). Rather, this discrepancy may indicate that an intra-continental boundary, if it does exist and is marked by the NSGL on the surface (Griffin et al., 1998; Menzies and Xu, 1998; Zheng et al., 2006; Xu, 2007), dips eastward at lithospheric depths (Chen et al., 2009).

The second-order feature is that the lithosphere is thinnest (~60–70 km) along the great strike-slip Tanlu Fault Zone near the eastern margin of the NCC, and thickest (up to ~200 km) under the stable Ordos Plateau within the continental interior, in agreement with their respective geographic locations, evolution histories and Phanerozoic tectonic activity. The third-order feature, and the most interesting one that has not been reported previously, is that rift areas, including not only the North China rift system in the eastern NCC but also the Shaanxi–Shanxi and Yinchuan–Hetao rift systems in the central and western NCC, all appear to be underlain by a significantly thinned lithosphere less than 100 km thick (profiles E–E′ and F–F′ in Fig. 3b and Fig. 4). The fourth-order feature, which directly relates to the above two features, is the dramatic variation of the lithospheric thickness on the western side of the NSGL, especially between the stable Ordos Plateau (≥200 km) and the surrounding Cenozoic rift areas (80–100 km). Most remarkably, a reduction of more than 100 km in the LAB depth occurs over a distance of ~200 km from the Ordos Plateau in the south to the Yinchuan–Hetao rift system in the north (Fig. 4; compare profiles F–F′ with G–G′ in Fig. 3b).

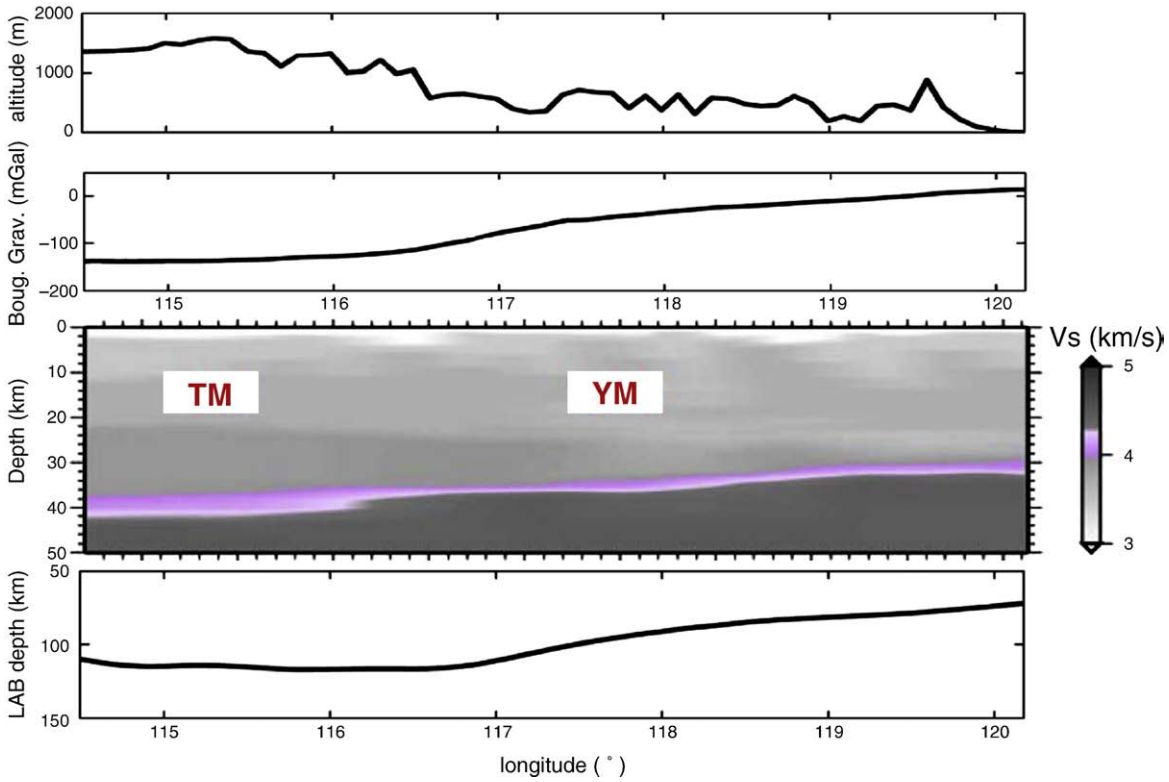

Fig. 5. Surface topography, Bouguer gravity anomaly, crustal shear velocities (Zheng et al., 2008a) and depth distribution of the LAB along a profile crossing the Yan Mountains (YM) and Taihang Mountains (TM) from east to west (thick white line in Fig. 4). The pink area in the shear velocity image represents the crust–mantle transition zone.

All these features suggest that the base of the lithosphere under the NCC probably has been re-shaped by the same regional tectonic processes that dominantly affected the present-day surface geology.

4.2. Crustal structure, lithospheric thickness and upper mantle anisotropy

The lithospheric thickness of the NCC also shows a close correlation with the crustal structure and upper mantle seismic anisotropy of the region, both of which display distinct features consistent with the three-fold subdivision of the craton (Zhao et al., 2008; Zheng et al., 2009). In general, the eastern NCC has a thin crust and lithosphere (<35 km and <100 km, respectively) and a WNW–ESE trending orientation of faster shear waves that travel nearly vertically through the mantle. On the other hand, the central and western NCC are characterized by a relatively thicker and structurally complex crust and lithosphere (Figs. 4, 5 and 6). The anisotropy pattern of the upper mantle in these regions is also significantly variable, with a mixture of NE–SW- and NW–SE-oriented fast directions and null splitting measurements of shear waves (Figs. 4 and 6b).

The changes in the crustal structure and upper mantle anisotropy also appear to be sharp, and concordant with the variation in lithospheric thickness near the boundary between the eastern and central NCC. For example, a large LAB step of ~40 km is detected near the junction between the Yan Mountains and the northern Taihang Mountains (Chen et al., 2008, profile F–F′ in Fig. 3b and Fig. 4), accompanying an abrupt change (nearly 90°) in the fast polarization direction of shear waves (Zhao and Zheng, 2005, Fig. 4). Almost at the same place but along an oblique profile (white solid line in Fig. 4) the structure of the crust–mantle boundary also varies significantly from a sharp interface beneath the eastern Yan Mountains to a transition zone up to 10 km thick under the western Taihang Mountains (Zheng et al., 2008a, Fig. 5). The variation in crustal structure is concordant with the changes of both Bouguer gravity anomaly and lithospheric thickness along the profile (Fig. 5), and also corresponds well to the variation in the trend of the two mountain belts (thin gray lines in Fig. 4). Similar concordant structural changes are also observed to the south around the boundary between the Bohai Bay Basin and the Taihang Mountains (profile E–E′ in Fig. 3b and Fig. 4), where a rapid thickening of the lithosphere coincides with an obvious deepening of the Moho discontinuity (more clearly seen in Fig. 6a), a marked change in the structure of the crust–mantle boundary and a sharp drop in Bouguer gravity anomaly (Zheng et al., 2006).

The structural variations may reflect different properties of the lithosphere in these areas. Detailed seismic structure-based gravity modeling suggests that the change in crustal structure along the basin-mountain profile (E–E′ in Fig. 3b) may not be sufficient to produce the observed gravity decrease, and a contribution from the underlying lithospheric mantle is required (Zheng et al., 2006). Both the seismic and the gravity data require a thicker and more buoyant lithospheric keel beneath the western mountain range, consistent with mantle xenolith data that imply at least a partial preservation of the refractory mantle root in the central NCC compared to the largely thinned and fertile lithospheric mantle in the eastern NCC (e.g., Zheng et al., 2001; Rudnick et al., 2006; Tang et al., 2006).

The marked heterogeneities among the Taihang Mountains, Yan Mountains and Bohai Bay Basin appear to be correlated with their different surface geological features, and Phanerozoic (and probably earlier) tectonics (Zheng et al., 2007, 2008a). This suggests that structures from the surface to the base of the lithosphere have evolved and deformed in a coupled way in both the interior and northern boundary of the eastern NCC and the eastern part of the central NCC. However, between these regions, the lithosphere appears to have mechanically decoupled and/or evolved under different tectonic regimes during the reactivation and destruction of the craton.

While the structural changes are mainly E–W in regions to the east of the NSGL including near the boundary between the eastern and central NCC, E–W and even more significant N–S variations in lithospheric structure are present on the western side of the NSGL. In

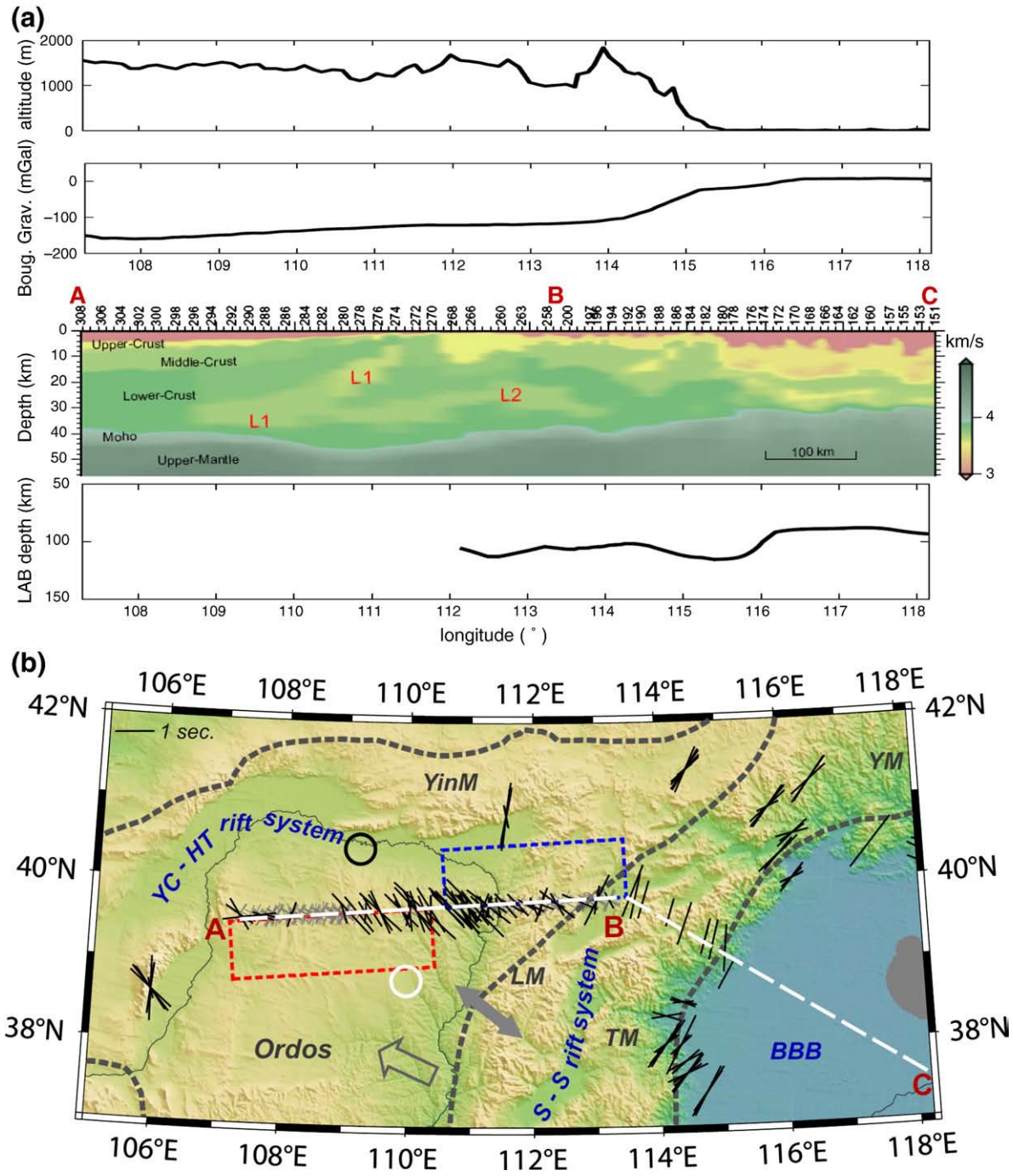

Fig. 6. (a) Surface topography, Bouguer gravity anomaly, crustal shear velocities (Zheng et al., 2009) and depth variation of the LAB along the NCISP-II and IV seismic arrays (see Fig. 2 and b for array locations). Two low-velocity zones identified in the crust are labeled as L1 and L2, respectively. (b) Map of the northern part of the western NCC showing the SKS splitting measurements (Zhao and Zheng, 2005; Zhao et al., 2008) from Fig. 4. Black circle and blue rectangle denote areas that may be underlain by a thinned lithosphere; white circle and red rectangle mark areas with a probable thick lithosphere (>180 km), as suggested by S- and P-RF imaging (Chen et al., 2009). Double-headed arrow denotes the average Cenozoic regional extension direction from Zhang et al. (1998, 2003). Single-headed arrow gives the average direction of absolute plate motion.

particular, N–S changes are obvious in both the lithospheric images (Fig. 3b) and the LAB depth map (Fig. 4), including the sharp thinning of more than 100 km in lithospheric thickness from the Ordos to the Yinchuan–Hetao rift system in the western NCC and the undulation of the LAB from ~140–180 km south of 38°N to <100 km farther north in the central NCC. These N–S variations in lithospheric structure were also suggested by recent surface wave tomography (Huang et al., 2009) and magnetotelluric surveys (Wei et al., 2008), and therefore probably represent robust structural features of the region. No concordant N–S variation in surface geology is observed in the central NCC except for slightly different rift morphology (Fig. 3a). A better understanding of this structural disharmony requires a thorough comparison among different parts of the central NCC; this is currently hindered by a lack of data, especially for areas to the south of the study region.

Due to this paucity of data, no detailed N–S comparison of the crustal structure and upper mantle anisotropy has been made for regions west of the NSGL. On the other hand, both the P-RF imaging

results (Zheng et al., 2006, 2009) and SKS splitting measurements (Zhao and Zheng, 2005; Zhao et al., 2008) from the dense NCISP-II and IV array data show concordant E–W changes in the shear velocity structure of the crust and the anisotropy pattern of the upper mantle (including both magnitude and direction) from the central to the western NCC (Fig. 6a and b).

The central part of the craton is characterized by significantly undulating intra-crustal interfaces and a generally NE–NNE orientation of faster shear waves, sub-parallel to the trend of Late Archean–Paleoproterozoic basement structures and Mesozoic mountain belts (thin gray lines in Fig. 4). Both features may be indicative of E–W to NWW–SEE compressive deformation associated with either the Paleoproterozoic amalgamation between the eastern and western NCC, or the Late Mesozoic extensional orogenic event that produced the Taihang Mountains coeval with the lithospheric rejuvenation in the eastern NCC, or both (Zhao and Zheng, 2005; Zhao et al., 2008; Zheng et al., 2009).

Around the boundary between the central and western NCC, the Moho rises slightly and a low-velocity anomaly appears in the lower crust (Fig. 6a), coinciding with the change in the fast direction of shear waves from coherent NNE in the eastern Taihang Mountains to a complex pattern/weak NW in the western area immediately to the north of the Lüliang Mountains (Fig. 6b). These variations may imply a transition in the tectonic deformation regime in the boundary region (Zhao et al., 2008), probably involving both the crust and the upper mantle.

An E–W structural variation is even more pronounced along the NCISP-IV seismic array in the western NCC. Distinct low-velocity zones in the crust (L1 and L2 in Fig. 6a) correspond to the strongest NW–SE anisotropy in the eastern portion of the array, whereas the well-stratified crustal structure corresponds to the weak anisotropy or null measurements of shear wave splitting to the west within the Ordos Plateau (Fig. 6a and b). Although the E–W change in the lithospheric thickness along the NCISP-IV array cannot be assessed using the S-RFs alone (with a gap shown in Fig. 4) because of a lack of S-RF sampling directly beneath the seismic array (see Sp piercing point distribution in Fig. 3a), detailed analyses and imaging of the P-RF data by wave equation migration do reveal different sub-Moho structural features in the eastern and western portions of the array (Chen et al., 2009). Comparisons between the migrated P- and S-RF images further suggest that the rapid reduction in lithospheric thickness may take place further north in the west than in the east and probably is sharper locally, corresponding to the arcuate shape of the geologically defined boundary between the Ordos Plateau and the Yinchuan–Hetao rift system (Fig. 6b, Chen et al., 2009).

4.3. The Ordos Plateau and surrounding region

The most intriguing feature revealed seismically is perhaps the fine-scale structural changes along both the E–W and N–S directions around the northeastern boundary of the Ordos Plateau (Figs. 3b, 4 and 6). Based on the structural images and available information on the geology, seismicity and regional tectonics, I have made detailed investigations on the relationship between the deep structure and surface tectonics and conducted further comparisons with the southern boundary of the Ordos Block and some other cratonic regions worldwide.

Around and to the south of the westernmost portion of the NCISP-IV array which lies within the Ordos Plateau, the imaged stratified crust and flat Moho (Fig. 6a), thick lithosphere (profile G–G′ in Fig. 3b and Fig. 4), and weak to null upper mantle anisotropy (Figs. 4 and 6b) all characterize a stable continental region with little detectable deformation or a vertically frozen mantle fabric (e.g., Petitjean et al., 2006). These observations agree with the relatively low heat flow (Wang et al., 1996; Hu et al., 2000), lack of volcanism and rare seismicity of the Ordos (Fig. 2), and probably reflect the minor influence of the later tectonic events on the cratonic nucleus of the western NCC.

To the east, in the middle-to-eastern segment of the array, the area close to the boundary between the Ordos Plateau and the Yinchuan–Hetao rift system (Fig. 6b) is characterized by pronounced low-velocity zones, thickened crust and an abrupt increase in the magnitude of upper mantle anisotropy, linked to a marked change in lithosphere thickness. A similar transition from weak or null to significant anisotropy is also observed between the Ordos Plateau and the Shaanxi rift area near the southern margin of the western NCC (Huang et al., 2008). The strong E–W upper mantle anisotropy in the Shaanxi rift system and the Qinling Orogen further south was suggested to be a result of both the Triassic collision of the NCC with the Yangtze Craton and the eastward upper mantle flow driven by the Cenozoic India–Eurasia collision (Huang et al., 2008).

However, the interpretation of the marked structural change around the northern boundary of the Ordos is still debated. By comparing the crustal shear velocity structure and anisotropy pattern of the upper mantle with the newly proposed Paleoproterozoic evolution model of the NCC (Faure et al., 2007), Zhao et al. (2008) and Zheng et al. (2009) suggested that the structure probably preserves the imprints of the Paleoproterozoic amalgamation process between the eastern and western NCC. Alternatively, the agreement between the observed NW–SE fast polarization direction of shear waves and the direction of the Cenozoic-to-present regional extension and the absolute plate movement direction (Fig. 6b) suggests that the structural change may be a result of more recent lithospheric processes. The pronounced anisotropy around the boundary between the Ordos Plateau and the Yinchuan–Hetao rift area probably represents vertically coherent deformation in the crust and upper mantle, possibly associated with the tectonic reactivation and/or thinning of the lithosphere under the circum-Ordos rift systems, similar to that suggested for the southern margin area of the Ordos Plateau (Huang et al., 2008). The complex pattern of anisotropy further to the east in areas north of the Lüliang Mountains and around the northern part of the Shanxi rift system (Fig. 6b) thus may reflect the interplay between this tectonic regime and the one that dominated upper mantle deformation in the Taihang Mountain region.

Whatever the cause, the sharp structural variations (both E–W and N–S) around the NCISP-IV array indicate substantial heterogeneity and complicated tectonic deformation at depth, which deserve further investigation. More seismic data and deep structural imaging, multi-disciplinary analysis and systematic comparisons over a broader region are required to elucidate the essential characteristics and the origin of the structural heterogeneity and its relation with regional tectonics.

Rapid changes in lithospheric structure like those seen in the western NCC also are observed in several other continental regions, mostly near the boundaries of cratons. Examples include the Sorgenfrei–Tornquist Zone bordering the eastern European craton (e.g., Shomali et al., 2006), the Baikal rift area around the southern boundary of the Siberian craton (Lebedev et al., 2006), and areas between tectonic blocks of different ages (including Archean) in continental Australia (Fishwick et al., 2008). All of these areas show structural variations comparable to, or even sharper than, that observed near the northern boundary of the western NCC. Recent geodynamic modeling results suggest that viscosity contrasts are crucial in preserving such a strong short-scale lithospheric heterogeneity against thermomechanical erosion by active mantle convection (Hieronymus et al., 2007). This explains why sharp variations in lithospheric structure are mostly found at the boundaries of cratonic regions, where the low temperature and distinct composition of the cratonic mantle provides a high viscosity. A change in the properties of the lithosphere therefore may account for the rapid structural change between the Ordos Plateau and the Yinchuan–Hetao rift system immediately to the north. This explanation may also be applicable to the part of the Shaanxi–Shanxi rift system that is underlain by a significantly thinned lithosphere (Fig. 4) and probably also to the other cratonic boundary regions mentioned above.

The rifting systems surrounding the Ordos and the Yin Mountains further to the north had originally been cratonic in nature as a part of the NCC, as indicated by examination of the lithology, geochemistry, geochronology, structure and metamorphism in the exposed Archean-to-Paleoproterozoic basement of the region (Zhao et al., 2001, 2005). The presence of significantly thinned lithosphere at the present time (Fig. 4, Chen et al., 2009; Huang et al., 2009) together with the active Cenozoic tectonics and seismicity in these regions (Fig. 2) indicates that at least some boundary regions including ancient collisional zones in the western and central NCC have experienced lithospheric reactivation and thinning. This corroborates recent petrological and geochemical observations (e.g., Xu et al., 2004a; Tang et al., 2006; Xu, 2007) that mantle xenoliths from around the rift areas west of the NSGL differ isotopically and chemically from both the "young" and fertile Cenozoic-to-present mantle lithosphere of the eastern NCC and the typical "old" and refractory roots found beneath cratons worldwide. Collectively, all these suggest that the lithospheric reactivation and thinning of the NCC might have affected a larger geographic region than previously thought. To the west of the NSGL, it may have been initiated at the boundaries of the Archean nucleus under the Ordos Plateau, but probably have not affected the very core of the craton.

5. Lithospheric thickness *vs* mantle transition zone thickness

The distinct structural features from the surface to the base of the lithosphere, probably also including the deformed shallow upper mantle in the NCC, certainly reflect the long-term tectonic evolution of the craton, which is closely tied to mantle dynamics. It has been long debated which dynamic processes or deep events caused the Phanerozoic lithospheric reactivation and thinning of the NCC and were responsible for the observed structural features. To tackle this issue, we need detailed knowledge about the structure of the mantle transition zone, which is important in the context of plate tectonics and mantle dynamics. The thickness of the mantle transition zone has often been taken as an indicator of the temperature regime in the upper mantle (e.g., Revenaugh and Jordan, 1991; Owens et al., 2000; Lebedev et al., 2002; Li and Yuan, 2003) which serves as a link between mantle dynamics and regional tectonics. To relate the Phanerozoic lithospheric thinning to the deeper mantle processes under the NCC, we can compare the lithospheric thickness estimated from S-RF images with the mantle transition zone thickness recently derived by P-RF migration (Chen and Ai, 2009).

These two thicknesses appear to be generally anti-correlated on the opposite sides of the NSGL (compare Fig. 7a with 7b). To the east, a much thinned lithosphere of 60–100 km corresponds to a thicker mantle transition zone of >250 km up to ~290 km. To the west, a relatively thicker lithosphere (mostly >120 km except for the two rift systems) is underlain by a normal-to-thin transition zone 235–250 km thick. Like the change in lithospheric thickness (and surface geology, crustal structure and upper mantle anisotropy), the change in the thickness of the mantle transition zone between the two domains also appears to be relatively sharp, and occurs close to the boundary between the eastern and central NCC and east of the NSGL (circles in Fig. 7b). Interestingly, this change in thickness also coincides with an obvious variation in the structural features of the lower boundary of the mantle transition zone (the 660-km discontinuity), whereas the upper boundary (the 410-km discontinuity) is structurally simple and relatively constant in depth (Fig. 8, Chen and Ai, 2009).

The thicknesses of the mantle transition zone and the lithosphere also exhibit smaller-scale variations that apparently deviate from this general anti-correlation. One example is found in the northern part of the western NCC. The thickness of the mantle transition zone drops from ~250 km beneath the Ordos Plateau to ~240 km and even as low as ~235 km in the Yinchuan–Hetao rift system and the Yin Mountains (Fig. 7b); this variation is similar to but much less pronounced than the N–S change in lithospheric thickness (Fig. 7a). A similar change is observed between the Ordos Plateau and the Shanxi rift system in the central NCC, although the magnitude of variation is smaller. Given the significantly thinned lithosphere and active Cenozoic tectonics of the circum-Ordos region, the correlation between the thicknesses of the mantle transition zone and the lithosphere is probably not fortuitous, and may reflect a direct correlation between shallow lithospheric processes and deeper mantle dynamics.

The thickness and discontinuity structure of the mantle transition zone (Figs. 7b and 8) provide information about the thermal regime in the deep upper mantle beneath the NCC. According to mineral physics data, the observed seismic discontinuities bounding the mantle transition zone are primarily associated with the transformations of olivine to wadsleyite (~410 km) and ringwoodite to perovskite + magnesiowustite (~660 km) (Ringwood, 1991; Bina and Helffrich, 1994; Fei et al., 2004). In most cases, lower (higher) temperatures will cause thickening (thinning) of the mantle transition zone because of the opposite Clapyron slopes of the 410- and 660-km phase transitions. The map of the mantle transition zone thickness of the NCC (Fig. 7b) therefore suggests a cool thermal regime to the east of the NSGL and a normal-to-warm regime to the west. This is consistent with recent tomographic results that show a high-velocity slab — probably the cold Pacific plate — trapped in the mantle transition zone beneath eastern China, with the western edge of the slab roughly coinciding with the NSGL (Huang and Zhao, 2006). Moreover, the complex structural features of the 660-km discontinuity (e.g., Fig. 8) and the distinct differences between the southern and northern parts of the eastern NCC (Huang and Zhao, 2006; Chen and Ai, 2009, e.g., Fig. 7b) probably are related to the complex morphology and subduction pattern of the Pacific slab, and associated temperature variations beneath this region (Chen and Ai, 2009).

On the other hand, both the generally thinned crust (Li et al., 2006; Zheng et al., 2006, 2008a,b) and lithosphere (Fig. 7a, Chen et al., 2006a, 2008) as well as relatively high heat flow (Hu et al., 2000) suggest a rather warm shallow upper mantle under the eastern NCC. In contrast, a thicker crust (Li et al., 2006; Zheng et al., 2006, 2009; Chen, 2009) and lithosphere (Fig. 7a, Chen et al., 2009) and lower heat flow (Wang et al., 1996; Hu et al., 2000) are found on the western side of the NSGL, reflecting a relatively cool environment in the shallow upper mantle of the region.

These observations indicate that the shallow and deep upper mantle on the two sides of the NSGL probably have not reached thermal equilibrium at the present time. In particular, the presence of the stagnant Pacific slab at the bottom of the upper mantle and the nearly flat structure of the 410-km discontinuity (Fig. 8, Chen and Ai, 2009), suggest that the Cenozoic lithospheric tectonics and magmatism in the eastern NCC have originated within the shallow upper mantle, possibly no deeper than the upper boundary of the mantle transition zone. To the west, the locally correlated thinning of both the lithosphere and mantle transition zone implies a warm regime in both the shallow and deep upper mantle. This suggests that the Cenozoic crustal rifting in areas surrounding the Archean nucleus of the western NCC is a manifestation of a late thermal event that affected the entire upper mantle of the region.

6. Different tectonic regimes across the NSGL

These structural comparisons strongly suggest a close correlation between mantle dynamics, lithospheric tectonics and surface geology on the two sides of the NSGL. The contrasting structural features of the two domains may reflect different thermal and/or chemical properties, different deep processes and different tectonic regimes that have dominated the evolution of these regions in the Phanerozoic.

6.1. East — effects of the Pacific subduction

Many lines of evidence, including the seismic images presented here, show that the cratonic lithosphere of the eastern NCC (to the

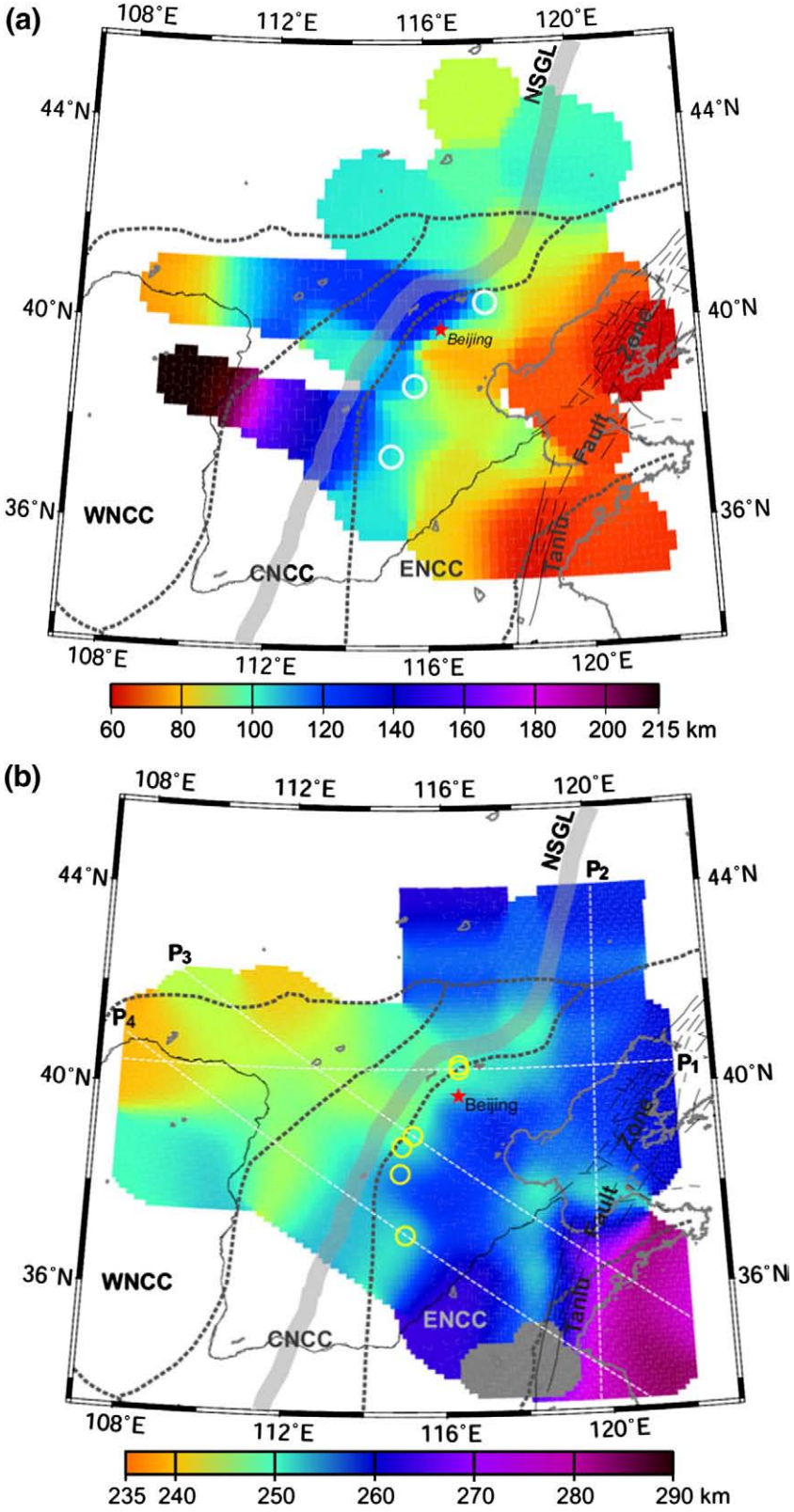

Fig. 7. Comparison between the maps of (a) lithospheric thickness from Fig. 4 with a slightly different latitude range and (b) mantle transition zone thickness (modified from Fig. 8 of Chen and Ai, 2009) across the study region. White circles in a mark the locations along profiles E–E′, F–F′ and G–G′ (as indicated by black arrows in Fig. 3b) at which a sharp change is observed in lithospheric thickness, upper mantle anisotropy, crustal structure and surface geology; yellow circles in b mark the locations where a rapid variation is detected in the thickness of the mantle transition zone and in the structure of the 660-km discontinuity. Dark gray color in b defines the area where double 660-km discontinuities are observed.

east of the NSGL) has been largely, if not fully, modified or destroyed probably mostly during the Late Mesozoic. Modeling studies suggest that cratonic lithosphere can be thinned significantly by thermo-mechanical erosion from mantle convection, but only over timescales of ≥2 Ga (Lenardic and Moresi, 1999; King, 2005; Hieronymus et al., 2007). Even by directly interacting with a hot mantle plume,

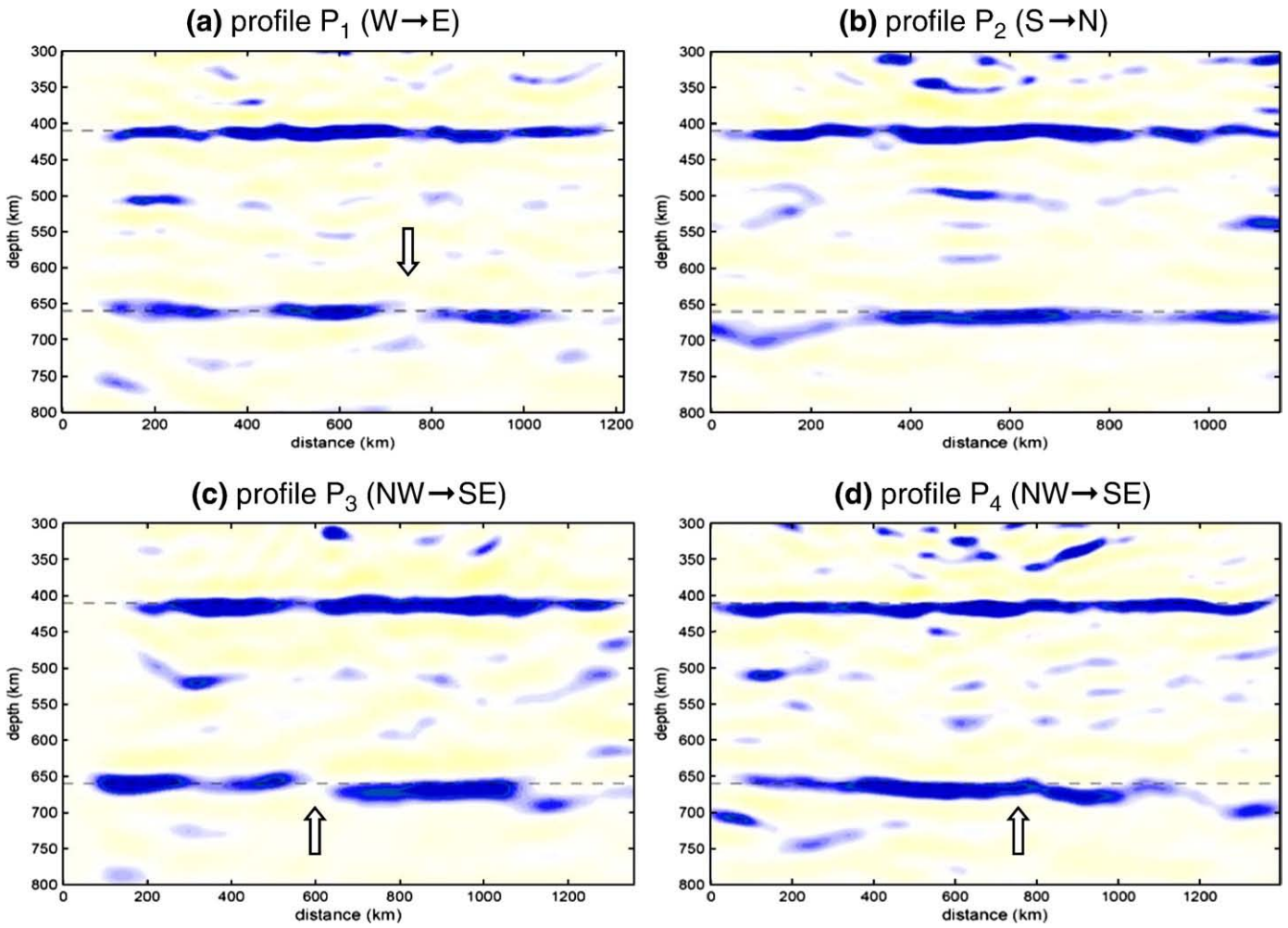

Fig. 8. Migrated P-RF images along the four profiles shown as white dashed lines in Fig. 7b (after Chen and Ai, 2009). Those in (a, b, and d) are constructed within a frequency range of 0.03–0.4 Hz, and that in c within 0.03–0.3 Hz because of higher noise level. Black dashed lines in each panel mark 410- and 660-km depths. Open arrows mark the rapid changes in mantle transition zone thickness and in the structure of the 660-km discontinuity near the boundary between the eastern and central NCC (yellow circles in Fig. 7b).

erosion of a thick Archean lithosphere is only possible when the craton is anchored above the plume for a long period of time (probably >200 Ma, Petitjean et al., 2006). However, in the eastern NCC there is no evidence for such plume activity (e.g., Zhang and Tanimoto, 1993; Wu et al., 2005; Huang and Zhao, 2006). Therefore, the destruction of the cratonic lithosphere in the eastern NCC is unlikely to reflect thermomechanical erosion either from mantle convection (such as induced by LAB topography, Hieronymus et al., 2007) or from hot plumes. Instead, it would require processes that disturbed the mantle convection pattern and the physical and chemical equilibrium between the lithosphere and the underlying mantle.

The dynamic trigger for such processes must have come from past tectonic events that affected the NCC. Although several such events may have contributed to the reactivation of the cratonic lithosphere, a number of authors have proposed that the deep subduction of the Pacific plate underneath East Asia since Mesozoic played a pivotal role in the destruction of the eastern NCC (e.g., Griffin et al., 1998; Wu et al., 2003a; Zhao et al., 2007a,b; Zhu and Zheng, 2009). This argument is based mainly on the similar timing of the two events, most remarkably during the Early Cretaceous (120–130 Ma), a period of peak lithospheric thinning of the region characterized by major magmatism (Xu et al., 2004b; Wu et al., 2005), intensive tectonic extension (Ren et al., 2002) and large-scale gold mineralization (Yang et al., 2003; Sun et al., 2007). The predominant trench-parallel NE–SW trending directions of both the extensional structures (Tian et al., 1992; Ren et al., 2002) and the two major elongated tectonic zones — the NSGL and the Tanlu Fault Zone in east China (Fig. 1a) — also favor the Pacific-regime interpretation.

Our seismic images of the deeper structure derived from dense-array data, together with recent high-resolution tomographic images (Huang and Zhao, 2006), lend further support to this interpretation. There is a close correspondence between the imaged morphology of the stagnant Pacific slab (Huang and Zhao, 2006) and the variations in the thickness and discontinuity structure of the mantle transition zone (Figs. 7b and 8), as well as the changes in crustal and lithospheric structure, gravity field and surface geology in the NCC (Figs. 3–6). Furthermore, the agreement between the NW–SE fast polarization direction of shear waves in this region (Zhao and Zheng, 2005) and the direction of back-arc extension arising from the Pacific subduction (e.g., Ratschbacher et al., 2000, Fig. 4) suggests that the present-day lithosphere beneath the eastern NCC retains a record of the Late Mesozoic to Early Cenozoic tectonic deformation. These observations, combined with the coherent timing, therefore suggest that the deep subduction of the Pacific plate may have been the most important influence on the Phanerozoic mantle dynamics and tectonic evolution of the eastern NCC.

The effects of Pacific-plate subduction may be manifold. In addition to the commonly proposed back-arc lithospheric extension and production of a thermal anomaly (e.g., Ye et al., 1987; Stuart et al., 1991; Ren et al., 2002; Zhang, 2007), the Pacific-plate subduction would also continuously release water-rich fluids at various depths by

dehydration reactions in the slab (Omori et al., 2004; Ohtani et al., 2004; Komabayashi et al., 2004) and induce vigorous convective circulation in the upper mantle wedge (e.g., Lei and Zhao, 2005; Zhao et al., 2007a,b). The subduction rate of the Pacific plate probably increased in the Early Cretaceous (Wu et al., 2005), due to either the uprising of the mid-Pacific superplume (Larson, 1991) and/or a mantle avalanche related to the closure of Tethys (Machetel and Humler, 2003) or the breakup of Gondwana (Wilde et al., 2003). Such an escalation of subduction would transport water to great depths, even into the mantle transition zone, by facilitating deeper dehydration of the slab, and induce upwelling of hot deeper mantle, which would further lead to extensive magmatism and rifting in eastern China. It also could disturb mantle convection, probably by intensifying thermomechanical and chemical erosion (including mantle–melt interaction) at the base of the overlying continental lithosphere and/or triggering gravitational instability and delamination of the modified lithosphere. Both processes, which are distinctly different from stable mantle convection, may have contributed to the destruction of the lithospheric root of the eastern NCC in the Late Mesozoic (e.g., Xu, 2001; Wu et al., 2003b; Gao et al., 2004; Zhang, 2005).

The influence of the Pacific-plate subduction may have weakened through the Cenozoic, probably because of the decrease in subduction rate (Engebretson et al., 1985; Northrup et al., 1995) and continuous trench retreat (Jolivet et al., 1994, 1999; Miller and Kennett, 2006). However, the structural features of the eastern NCC identified by the seismic studies suggest that the effects of subduction may persist to the present day, perhaps due to the flattening of the Pacific plate above the base of the upper mantle, forming a “big mantle wedge” in the region stretching from the northwestern Pacific to eastern Eurasia during the Cenozoic (Lei and Zhao, 2005; Huang and Zhao, 2006; Zhao et al., 2007a,b). The cool regime suggested by the observed thickening of the mantle transition zone is consistent with the cooling effect of the flat-flying Pacific slab at the bottom of the upper mantle, and a relatively hot shallow upper mantle may reflect subduction-induced upwelling of hot asthenosphere. Moreover, the simple and flat 410-km discontinuity imaged beneath this region (Ai and Zheng, 2003; Chen et al., 2006b; Chen and Ai, 2009, Fig. 8) implies weak and smooth variations in temperature and/or composition (such as water abundance) near the top surface of the stagnant slab. This probably is a consequence of the continuous convective circulation in the mantle wedge, which serves to quickly remove the slab-associated anomalies immediately above the stagnant slab. In contrast, the observed substantial topography and complex structural features of the 660-km discontinuity (Ai and Zheng, 2003; Chen and Ai, 2009, Fig. 8) correspond to significant thermal and/or chemical anomalies at the bottom of the slab, which may result from the direct interaction between the cold Pacific slab and the 660-km discontinuity.

6.2. West — role of pre-existing lithospheric structure

The influence of the Pacific subduction in regions to the west of the NSGL must have been limited, as suggested by the absence of widespread regional extension (Zhang et al., 1998, 2003), limited Eocene faulting and generally thin Oligocene rift-type sediments (Ye et al., 1987), and by the contrasts in structural features and thermal regimes of the upper mantle between the western and eastern parts of the NCC (e.g., Figs. 4 and 7).

The major differences in the magnitude of extension, morphology and Cenozoic tectonics in the extensional rift systems on the two sides of the NSGL suggest fundamentally different tectonic regimes during the Phanerozoic lithospheric deformation. In particular, extensional rifting in the west is restricted to the elongated zones surrounding the Ordos Plateau and did not extend to the whole periphery of the Ordos until late Neogene time, in contrast to the widespread rifting that continued from the Late Cretaceous to the Early Tertiary in the east (Zhang et al., 1998; Ren et al., 2002; Zhang et al., 2003). All these observations, together with the east-directed rollback of the Pacific plate and the possible eastward migration of subduction-associated tectonics in the Cenozoic (e.g., Jolivet et al., 1994, 1999; Miller and Kennett, 2006) make it improbable that the far-field effects of the Pacific subduction reached the western side of the NSGL, as proposed earlier (Yin, 2000).

The Phanerozoic lithospheric reactivation and thinning may not have affected the central and western NCC to the same extent as the eastern NCC. A large part of the cratonic lithosphere beneath these regions remains relatively thick today (Fig. 4). The mantle transition zone in the central and western NCC shows smoother structural features and weaker thermal anomalies than that in the eastern part of the craton (Fig. 7b, Chen and Ai, 2009), also suggesting a relatively weak effect of mantle dynamics on the Cenozoic tectonics of the central and western parts of the craton. However, boundary zones around the cratonic nucleus may have undergone lithospheric reactivation and deformation, as indicated by the significantly thinned lithosphere, extensional rifting, magmatism, active faulting and seismicity surrounding the Ordos Plateau (Figs. 1b, 2b and 4, Zhang et al., 1998, 2003).

Both of the rift systems on the western side of the NSGL correspond to pre-existing structures in the cratonic lithosphere. The Yinchuan–Hetao rift system is close to the northern boundary of the western NCC and roughly coincides with the EW-trending Paleoproterozoic Khondalite Belt (Fig. 1b), which sutured the Ordos Block and the Yinshan Block to form the western NCC (Zhao et al., 2003). The Shaanxi–Shanxi rift zone is within the Trans-North China Orogen, which resulted from the collision between the eastern and western NCC ~1.85 Ga ago (Zhao et al., 2001, 2005). These ancient collisional or orogenic belts probably are mechanically weak compared with the adjacent cratonic nucleus, and probably have been so ever since their formation in the Paleoproterozoic.

Pre-existing structures in the lithosphere can function as the primary control on the tectonothermal evolution of the continental regions. Mineral physics experiments and numerical modeling suggest that such pre-existing structures may induce a significant anisotropy in thermal diffusivity (Tommasi et al., 2001) and mechanical deformation (Tommasi and Vauchez, 2001) in the uppermost mantle. This anisotropic behavior can lead to anisotropic heating and strain localization within the lithosphere, thus favoring the reactivation of the ancient fabric during later tectonothermal events (Vauchez et al., 1997; Tommasi et al., 2001). Such effects have been inferred, for instance, in the east African rift (Achauer and KRISP working group, 1988; Keranen and Klemperer, 2008), SE Brazil (James and Assumpção, 1996), the eastern United States (Barruol et al., 1997), the Baikal rift (Lesne et al., 2000) and the Kalahari craton in Southern Africa (Savage and Silver, 2008).

The ancient structural belts around the Archean Ordos may have been repeatedly reactivated in a similar way by successive tectonic events during the long-term evolution of the NCC. In particular, the Paleoproterozoic Khondalite Belt and the northern boundary regions of the NCC probably were affected by the progressive subduction of the Paleo-Asian ocean and the amalgamation of terranes that produced the Central Asian Orogenic Belt in Paleozoic to early Mesozoic time (Buslov et al., 2001; Badarch et al., 2002; Xiao et al., 2003). The northern boundary of the NCC was an active continental margin during that period (Xiao et al., 2003; Zhang et al., 2007), and its lithosphere might have already been weakened, deformed and even thinned, probably with a relatively sharp change in structure (perhaps including thickness) and properties from the cratonic interior to the margins after the final collision with the Siberia craton and post-collisional uplift. This would be more likely to take place in the western part of the NCC because of its proximity to the suture zone and/or the presence of the ancient collisional Khondalite Belt. The northern boundary area of the orogenic belt in the central NCC may also have been affected by this event.

The India–Eurasia collision has been proposed as a major influence on the lithospheric tectonics of the central and western NCC during Cenozoic time (e.g., Menzies et al., 1993; Liu et al., 2004; Deng et al., 2004; Xu, 2007); Ren et al. (2002) suggested that the dominant NW–SE-trending Cenozoic-to-present extension of the region was induced by the rapid convergence of India–Eurasia relative to Pacific–Eurasia. Deformation of the crust and probably the lithospheric mantle around the Ordos Plateau resulting from this NW–SE extension may have been accompanied by differential counterclockwise rotations between the Ordos and surrounding blocks (e.g., Zhang et al., 1998, 2003). These rotations probably also have contributed to the complexity of the upper mantle anisotropy pattern near the boundary between the Ordos and the two rift systems (Fig. 6b). The hotter mantle transition zone imaged near the northern margin of the western NCC and beneath areas in the central NCC (Fig. 7b) corresponds to the tomographically observed low-velocity structures in the shallow upper mantle (e.g., Liu et al., 2004; Huang and Zhao, 2006; Pei et al., 2007), which have been interpreted to represent a lateral asthenospheric mantle flow driven by the India–Eurasia collision (Liu et al., 2004). These observations suggest that the influence of the India–Eurasia collision, although relatively weak compared to that of the Pacific subduction on the eastern NCC, might have involved the whole lithosphere and even extended to the deep upper mantle. Since the thinned lithosphere in the central and western NCC spatially coincides with the Cenozoic extensional rifting systems, it is possible that the collision of the Indian plate with Eurasia may have further deformed the already weakened lithosphere under the pre-existing structural zones, intensified the structural contrast between them and the craton interior, and eventually caused rifting in these zones.

There are two possibilities for the lithospheric thinning to the west of the NSGL. One is that the pre-existing structure of the lithosphere was only weakened and deformed to some extent but not significantly thinned by the earlier events; lithospheric thinning mainly occurred in the Cenozoic, triggered by the inter-continental collision of India–Eurasia, much later than its eastern counterpart. Such a diachronous lithospheric thinning scenario has been suggested by Xu et al. (2004a) and Xu (2007) based primarily on petrological and geochemical data from mantle xenoliths in the northern part of the Shaanxi–Shanxi rift system. Our images of lithospheric structure and LAB topography in this area (profile E–E′ in Figs. 3b and 4) do not contradict this scenario.

Alternatively, the thinned lithosphere of the region, especially around the northern margin of the western NCC, and the sharp change in lithospheric structure from the Yinchuan–Hetao rift to the Ordos, may be ancient features produced by earlier tectonic events, most probably the Paleozoic to early Mesozoic formation of the Central Asian Orogenic Belt. With a combination of active mantle convection and compositional stabilization of the cratonic side (high viscosity and strength), the sharp structural change could have been maintained against convective erosion over timescales of hundreds of Ma. Hieronymus et al. (2007) have proposed a similar mechanism for the preservation of the ~150-km lithospheric step at the Sorgenfrei–Tornquist Zone bordering the eastern European craton, which has lasted at least 200 Ma.

The pre-existing structure and boundary zones in the eastern NCC, such as the Paleoproterozoic Jiao-Liao-Ji Belt and the northern and southern boundary regions, may also have suffered lithospheric reactivation and deformation by tectonic events before the Late Mesozoic lithospheric decratonization. The spatial coincidence of the Tanlu Fault Zone with the Jiao-Liao-Ji Belt (Fig. 1b) suggests that the Triassic collision of the NCC with the Yangtze Craton reactivated this ancient belt, leading to the formation of the Tanlu Fault Zone. Due to its inherited mechanical weakness, this fault zone may have been more significantly affected by the later Pacific subduction and associated processes than other regions in the eastern NCC; today it has the thinnest lithosphere within the entire craton (Fig. 4).

The stress field associated with the Triassic continental collision also may have destroyed the physical integrity of the lithospheric mantle beneath the southern NCC (not only in the eastern part), and facilitated the later reactivation and destruction of the craton (e.g., Xu, 2001). This has indeed been suggested by a number of geological, petrographic and geochemical studies on the southern marginal areas of the NCC including the Qinling-Dabie-Sulu orogenic belts (e.g., Fan et al., 2001; Zhang et al., 2002; Xu et al., 2004b; Zhang, 2007). However, more data and further studies, especially by using dense geophysical field observations will be required to understand how the present-day lithospheric structure varies from these marginal areas to the craton interior, and the relationship between the variations of shallow and deep structures.

6.3. Suggested tectonic model

Based on these multidisciplinary observations and the preceding discussion, it is possible to construct a tectonic evolution model for the lithospheric reactivation and thinning of the NCC, as shown in Fig. 9.

The ancient structural zones and marginal regions of the craton may have been weakened and deformed by successive tectonic events from the final cratonization of the NCC in the Paleoproterozoic to the early Mesozoic (Fig. 9a). Some of these areas, possibly including those around the northern boundary of the western NCC, may even have been thinned before the subduction of the Izanagi–Kula–Pacific plate under East Asia in the middle Mesozoic.

During the Late Mesozoic, mantle processes other than stable convection, probably including thermo–mechanical–chemical erosion and/or gravitational instability-induced lithospheric delamination, affected the eastern NCC. These processes were aided by the intensified subduction and deep dehydration of the Pacific plate and vigorous subduction-induced convective circulation in the mantle wedge. This led to voluminous magmatism, widespread extensional rifting and significant modification and destruction of both the already deformed (even thinned) boundary zones and the cratonic nuclei, giving rise to thinned lithosphere and crust and chemically fertile lithospheric mantle across the region (Fig. 9b). The central and western NCC were much less affected by the Pacific subduction, and the lithosphere under a large part of these regions may have remained relatively thick during the Mesozoic. The distinct Mesozoic tectonics in the different parts of the craton may have resulted in contrasting structural features from the surface to the base of the upper mantle under the eastern NCC and the central and western NCC, and eventually induced the development of an intra-continental boundary between these blocks, as marked by the NSGL on the surface (Fig. 9b).

The influence of the Pacific subduction on eastern China may have weakened through the Cenozoic (Fig. 9c). The beginning of the India–Eurasia collision from the southwest probably triggered lithospheric remobilization and thinning and extensional rifting along pre-existing weak zones in the central and western NCC. However, this collisional event seems to have had a smaller effect on the regional tectonics and may not have significantly disturbed the mantle convection under eastern China (Fig. 9c). The Cenozoic erosion of the lithosphere west of the NSGL therefore was much less than that in the eastern NCC during the Late Mesozoic (Fig. 9b), and lithosphere up to 200 km thick and generally thick crust could survive on the western side of the NSGL (Fig. 9c).

7. Concluding remarks

The integration of seismic images of structures at different depths with other geophysical observations and geological, petrographic and geochemical data enables systematic comparisons between different parts of the NCC and provides constraints on their respective tectonics in the Phanerozoic and even earlier. These comparisons show that

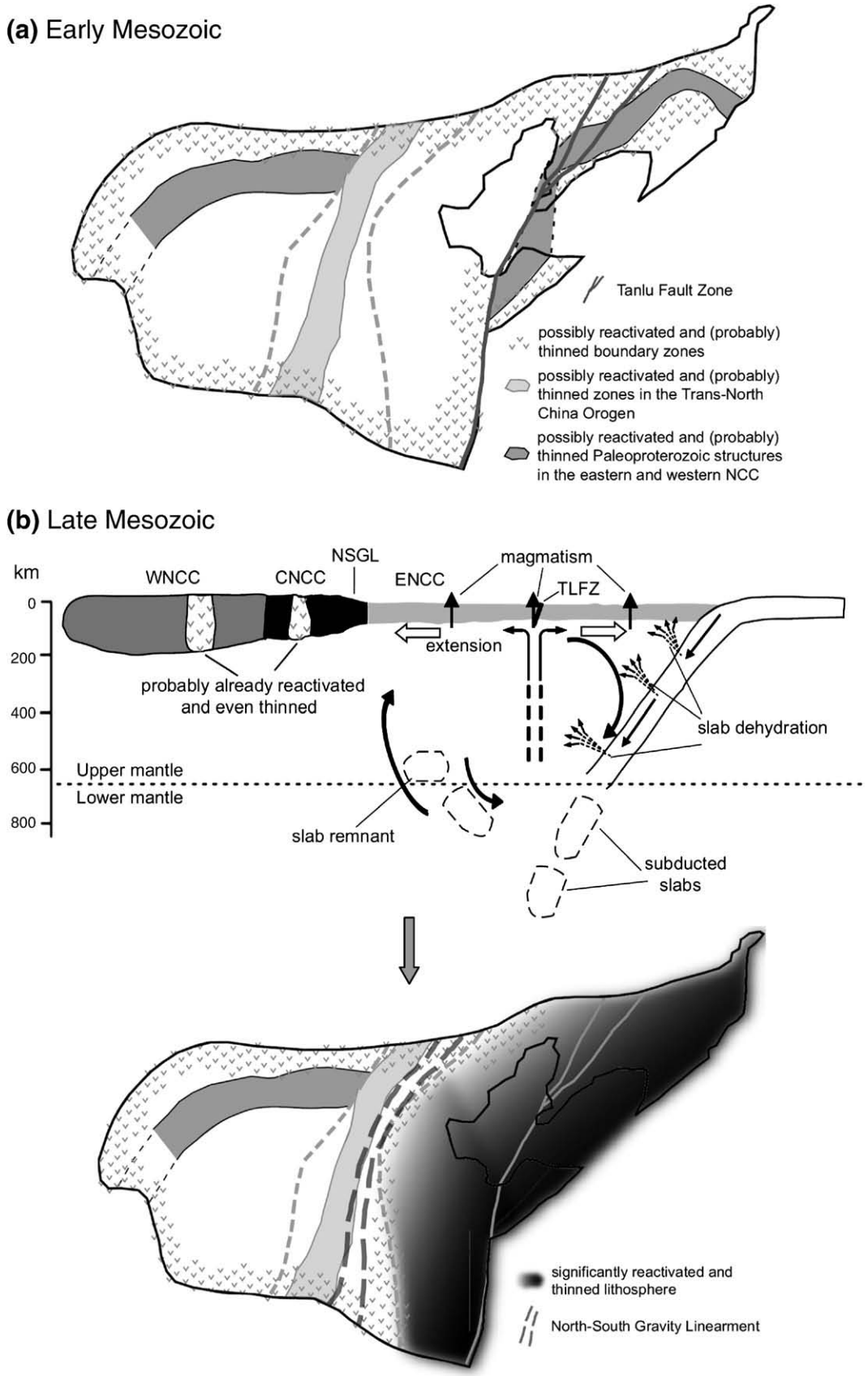

Fig. 9. Schematic illustration of the tectonic evolution of the NCC in the Phanerozoic. (a) Possibly weakened and deformed structural zones before the subduction of the Izanagi–Kula–Pacific plate under East Asia in the middle Mesozoic; (b) fundamental reactivation and destruction of the eastern NCC induced by the more vigorous deep subduction of the Pacific plate during Late Cretaceous; and (c) localized Cenozoic extensional rifting and lithospheric thinning along already weakened and deformed (probably also thinned) pre-existing lithospheric structures in the central and western NCC, caused by the India–Eurasia collision. Question marks denote regions for which there is still a lack of detailed deep structural information.

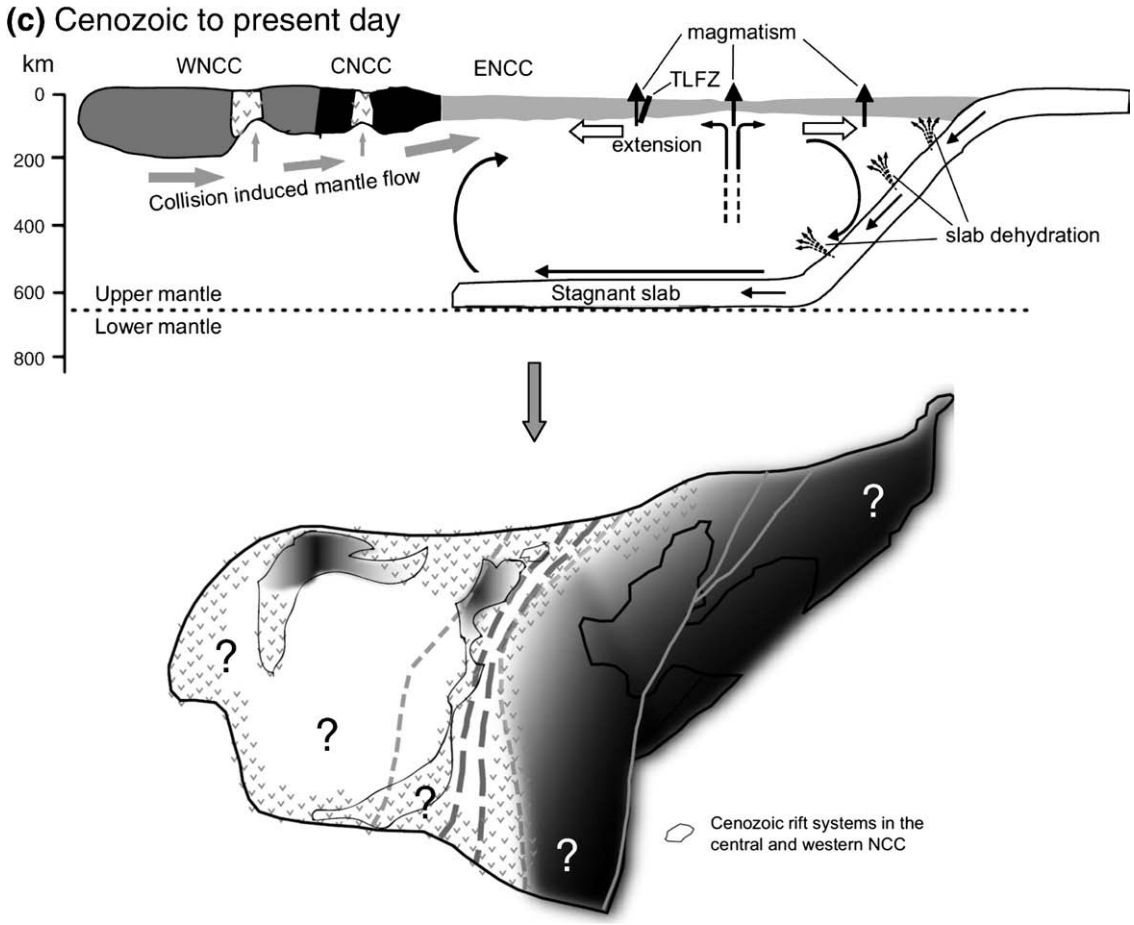

Fig. 9 (*continued*).

lithospheric remobilization and thinning may have affected the NCC much further to the west than previously thought, and that the structure varies concordantly from the surface down to the base of the upper mantle. In the eastern NCC the lithospheric reactivation is widespread and well-developed; in the central and western NCC only localized lithospheric modification and thinning have occurred.

These differences across the NSGL probably reflect different Mesozoic–Cenozoic lithospheric tectonics and mantle dynamics, working on pre-existing structures of the lithosphere in the two domains. The deep subduction of the Pacific plate from the east and associated processes may have dramatically changed the mantle dynamics and the physical and chemical state of the lithosphere in the eastern NCC since the middle Mesozoic, resulting in the reactivation and destruction of the cratonic lithosphere and related changes in surface tectonics and the deep structure of the region. The influence of the Pacific subduction appears to be insignificant in the central and western NCC. Instead, the India–Eurasia collision may have been the primary factor controlling the lithospheric tectonics of these regions in the Cenozoic. The effect of this event, however, probably was relatively weak, such that the mantle convection was not significantly disturbed, and lithospheric modification and thinning was less intensive and spatially more localized. In both domains, lithospheric reactivation appears to be more pronounced along ancient tectonic belts, in agreement with mineral physics experiments and numerical modeling that demonstrate the vulnerability of pre-existing lithospheric structures to tectono–thermal modification. These zones therefore have a significant function in the tectonic evolution of continents.

The NSGL extends ~4000 km N–S and separates the two distinct domains in the NCC; it also traverses northeastern China and southern China, and is accompanied along its length by a relatively rapid topographic change (Fig. 1a). One may be curious about what has happened underneath these other blocks to the north and south of the NCC. Tectonic extension was widespread in eastern China and adjacent regions in Late Mesozoic to Cenozoic time (Ren et al., 2002), forming the ~6000-km long Cenozoic extensional belt adjacent to the eastern margin of the Eurasian plate that includes the North China rift system in the eastern NCC (e.g., Northrup et al., 1995). The deep structural features and variation patterns in northeastern China and southern China, and their relationships with the NCC, are important for testing the tectonic models of the NCC proposed in this study and by others, and for a comprehensive understanding of the formation of the NSGL, the stabilization/destruction of the NCC and the Phanerozoic evolution of all of eastern China. This is an intriguing issue and will be investigated in detail by later research.

Acknowledgments

I thank the Seismic Array Laboratory in the Institute of Geology and Geophysics, Chinese Academy of Sciences and the China Earthquake Administration for providing the waveform data. I appreciate the help from Tianyu Zheng for providing the crustal structural images, Liang Zhao for providing the SKS splitting analysis results, Ya Xu for collecting the gravity data, Weijun Wang and Qifu Chen for providing the earthquake hypocenter data, and all the participants of the North China Interior Structure Project for their assistance in pre-processing the seismic waveform data. I am grateful to Rixiang Zhu for thoughtful discussions. Constructive reviews from William L. Griffin and two anonymous reviewers significantly improved the manuscript. This research is supported by the National Science Foundation of China (grant 90814002) and the Chinese Academy of Sciences.

References

Achauer, U., KRISP working group, 1988. New ideas on the Kenya rift based on the inversion of the combined dataset of the 1985 and 1989/90 seismic tomography experiments. Tectonophysics 236, 305–329.

Ai, Y., Zheng, T., 2003. The upper mantle discontinuity structure beneath eastern China. Geophysical Research Letter 30 (21), 2089. doi:10.1029/2003GL017678.

Badarch, G., Cunningham, W.D., Windley, B.F., 2002. A new terrane subdivision for Mongolia: implications for the Phanerozoic crustal growth of central Asia. Journal of Asian Earth Sciences 21, 87–110.

Barruol, G., Silver, P.G., Vauchez, A., 1997. Seismic anisotropy in the eastern United States: deep structure of a complex continental plate. Journal of Geophysical Research 102, 8329–8348.

Bartolini, A., Larson, R.L., 2001. Pacific microplate and the Pangea supercontinent in the Early to Middle Jurassic. Geology 29, 735–738.

Bina, C., Helffrich, G., 1994. Phase transition Clapeyron slopes and transition zone seismic discontinuity topography. Journal of Geophysical Research 99 (B8), 15,853–15,860.

Bruneton, M., Pedersen, H.A., Vacher, P., Kukkonen, I.T., Arndt, N.T., Funke, S., Friederich, W., Farra, V., SVEKALAPKO Seismic Tomography Working Group, 2004. Layered lithospheric mantle in the central Baltic Shield from surface waves and xenolith analysis. Earth and Planetary Science Letters 226, 41–52.

Buslov, M.M., Saphonova, I.Yu., Watanabe, T., Obut, O.T., Fujiwara, Y., et al., 2001. Evolution of the Paleo-Asian ocean (Altai-Sayan region, central Asia) and collision of possible Gondwana-derived terranes with the southern marginal part of the Siberian continent. Geoscience Journal 5, 203–224.

Chen, L., 2009. Lithospheric structure variations between the eastern and central North China Craton from S- and P-receiver function migration. Physics of the Earth and Planetary Interiors 173, 216–227.

Chen, L., Ai, Y., 2009. Discontinuity structure of the mantle transition zone beneath the North China Craton from receiver function migration. Journal of Geophysical Research 114, B06307. doi:10.1029/2008JB006221.

Chen, G.Y., Song, Z.H., An, C.Q., et al., 1991. Three dimensional crust and upper mantle structure of the North China region. Acta Geophysical Sinica 34, 172–181 (in Chinese with English abstract).

Chen, L., Zheng, T.Y., Xu, W.W., 2006a. A thinned lithospheric image of the Tanlu Fault Zone, eastern China: constructed from wave equation based receiver function migration. Journal of Geophysical Research 111, B09312. doi:10.1029/2005JB003974.

Chen, L., Zheng, T.Y., Xu, W.W., 2006b. Receiver function migration image of the deep structure in the Bohai Bay Basin, eastern China. Geophysical Research Letter 33, L20307. doi:10.1029/2006GL027593.

Chen, L., Wang, T., Zhao, L., Zheng, T.Y., 2008. Distinct lateral variation of lithospheric thickness in the Northeastern North China Craton. Earth and Planetary Science Letters 267, 56–68.

Chen, L., Cheng, C., Wei, Z., 2009. Seismic evidence for significant lateral variations in lithospheric thickness beneath the central and western North China Craton. Earth and Planetary Science Letters 286, 216–227.

Davis, G.A., Zheng, Y., Wang, C., Darby, B.J., Zhang, C., Gehrels, G., 2001. Mesozoic tectonic evolution of the Yanshan fold and thrust belt, with emphasis on Hebei and Liaoning provinces, northern China. In: Hendrix, M.S., Davis, G.A. (Eds.), Paleozoic and Mesozoic Tectonic Evolution of Central and Eastern Asia: Mem. Geol. Soc. Am., vol. 194, pp. 171–197.

Deng, J.F., Mo, X.X., Zhao, H.L., Wu, Z.X., Luo, Z.H., Su, S.G., 2004. A new model for the dynamic evolution of Chinese lithosphere: 'continental roots-plume tectonics'. Earth-Science Reviews 65, 223–275.

Engebretson, D.C., Cox, A., and Gordon, R.G., 1985. Relative motions between oceanic and continental plates in the Pacific Basin. Geological Society of America Special Paper 206, 59 p.

Fan, W.M., Zhang, H.F., Baker, J., Jarvis, K.E., Mason, P.R.D., Menzies, M.A., 2000. On and off the North China Craton: where is the Archaean keel? Journal of Petrology 41, 933–950.

Fan, W.M., Guo, F., Wang, Y.J., Lin, G., Zhang, M., 2001. Post-orogenic bimodal volcanism along the Sulu orogenic belt in eastern China. Physics and Chemistry of the Earth (A) 26, 733–746.

Farra, V., Vinnik, L., 2000. Upper mantle stratification by P and S receiver functions. Geophysical Journal International 141, 699–712.

Faure, M., Lin, W., Breton, N.L., 2001. Where is the North China–South China block boundary in eastern China? Geology 29, 119–122.

Faure, M., Trapp, P., Lin, W., Monié, P., Bruguier, O., 2007. Polyorogenic evolution of the Paleoproterozoic Trans-North China Belt—new insights from the Lüliangshan-Hengshan-Wutaishan and Fuping massifs. Episodes 30, 95–106.

Fei, Y., et al., 2004. Experimentally determined postspinel transformation boundary in Mg2SiO4 using MgO as an internal pressure standard and its geophysical implications. Journal of Geophysical Research—Solid Earth 109 (B2). doi:10.1029/2003JB002562.

Fishwick, S., Heintz, M., Kennett, B.L.N., Reading, A.M., Yoshizawa, K., 2008. Steps in lithospheric thickness within eastern Australia, evidence from surface wave tomography. Tectonics 27, TC4009. doi:10.1029/2007TC002116.

Freybourger, M., Gaherty, J.B., Jordan, T.H., Kaapvaal Seismic Group, 2001. Structure of the Kaapvaal craton from surface waves. Geophysical Research Letter 28, 2489–2492.

Gaherty, J.B., Kato, M., Jordan, T.H., 1999. Seismological structure of the upper mantle: a regional comparison of seismic layering. Physics of the Earth and Planetary Interiors 110, 21–41.

Gao, S., Rudnick, R.L., Carlson, R.W., McDonough, W.F., Liu, Y.S., 2002. Re–Os evidence for replacement of ancient mantle lithosphere beneath the North China Craton. Earth and Planetary Science Letters 198, 307–322.

Gao, S., Rudnick, R.L., Yuan, H.L., 2004. Recycling lower continental crust in the North China craton. Nature 432, 892–897.

Griffin, W.L., Zhang, A.D., O'Reilly, S.Y., Ryan, G., 1998. Phanerozoic evolution of the lithosphere beneath the Sino-Korean Craton. In: Flower, M., Chung, S.L., Lo, C.H., Lee, T.Y. (Eds.), Mantle Dynamics and Plate Interactions in East Asia: American Geophysics Union Geodynamics Series, vol. 27, pp. 107–126.

Gripp, A.E., Gordon, R.B., 2002. Young tracks of hotspots and current plate velocities. Geophysical Journal International 150, 321–361.

Hieronymus, C.F., Shomali, Z.H., Pedersen, L.B., 2007. A dynamical model for generating sharp seismic velocity contrasts underneath continents: application to the Sorgenfrei–Tornquist Zone. Earth and Planetary Science Letters 262, 77–91.

Hu, S., He, L., Wang, J., 2000. Heat flow in the continental area of China: a new data set. Earth and Planetary Science Letters 179, 407–419.

Huang, J., Zhao, D., 2006. High-resolution mantle tomography of China and surrounding regions. Journal of Geophysical Research 111, B09305. doi:10.1029/2005JB004066.

Huang, Z., Su, W., Peng, Y., Zheng, Y., Li, H., 2003. Rayleigh wave tomography of China and adjacent regions. Journal of Geophysical Research 108 (B2), 2073. doi:10.1029/2001JB001696.

Huang, Z., Xu, M., Wang, L., Mi, N., Yu, D., Li, H., 2008. Shear wave splitting in the southern margin of the Ordos Block, north China. Geophysical Research Letter 35, L19301. doi:10.1029/2008GL035188.

Huang, Z., Li, H., Zheng, Y., 2009. The lithosphere of North China Craton from surface wave tomography. Earth and Planetary Science Letters 288, 164–173.

James, D.E., Assumpção, M., 1996. Tectonic implications of S wave anisotropy beneath SE Brazil. Geophysical Journal International 126, 1–10.

Jolivet, L., Tamaki, K., Fournier, M., 1994. Japan Sea, opening history and mechanism; a synthesis. Journal of Geophysical Research 99, 22,237–22,259.

Jolivet, L., Faccenna, C., D'Agostino, N., Fournier, M., Worrall, D.M., 1999. The kinematics of backarc basins, examples from the Tyrrhenian, Aegean and Japan seas. In: MacNiocaill, C., Ryan, P.D. (Eds.), Continental Tectonics: Geological Society, London, Special Publications, vol. 164, pp. 21–53.

Karato, S.-I., Jung, H., 1998. Water, partial melting and the origin of the seismic low velocity and high attenuation zone in the upper mantle. Earth and Planetary Science Letters 157, 193–207.

Keranen, K., Klemperer, S.L., 2008. Discontinuous and diachronous evolution of the Main Ethiopian Rift: implications for development of continental rifts. Earth and Planetary Science Letters 265, 96–111.

King, S.D., 2005. Archean cratons and mantle dynamics. Earth and Planetary Science Letters 234, 1–14.

Komabayashi, T., Omori, S., Maruyama, S., 2004. Petrogenetic grid in the system MgO–SiO2–H2O up to 30 GPa, 1600 °C: applications to hydrous peridotite subducting into the Earth's deep interior. Journal of Geophysical Research 109, B03206.

Kusky, T.M., Windley, B.F., Zhai, M.-G., 2007. Tectonic evolution of the North China Block: from orogen to craton to orogen. Geological Society, London, Special Publications 280, 1–34.

Larson, R.L., 1991. Latest pulse of Earth: evidence for a mid-Cretaceous superplume. Geology 19, 547–550.

Larson, A.M., Snoke, J.A., James, D.E., 2006. *S*-wave velocity structure, mantle xenoliths and the upper mantle beneath the Kaapvaal craton. Geophysical Journal International 167, 171–186.

Lebedev, S., Chevrot, S., van der Hilst, R.D., 2002. Seismic evidence for olivine phase changes at the 410- and 660-kilometer discontinuities. Science 296, 1300–1302.

Lebedev, S., Meier, T., van der Hilst, R.D., 2006. Asthenospheric flow and origin of volcanism in the Baikal Rift area. Earth and Planetary Science Letters 249, 415–424.

Lei, J., Zhao, D., 2005. P-wave tomography and origin of the Changbai intraplate volcano in Northeast Asia. Tectonophysics 397, 281–295.

Lenardic, A., Moresi, L.-N., 1999. Some thoughts on the stability of cratonic lithosphere: effects of buoyancy and viscosity. Journal of Geophysical Research 104, 12,747–12,758.

Lesne, O., Calais, E., Deverchère, J., Chéry, J., Hassani, R., 2000. Dynamics of intracontinental extension in the north Baikal rift from two-dimensional numerical deformation modeling. Journal of Geophysical Research 105, 21,727–21,744.

Li, X., Yuan, X., 2003. Receiver functions in northeast China-implications for slab penetration into the lower mantle in northwest Pacific subduction zone. Earth and Planetary Science Letters 216, 679–691.

Li, S.G., Xiao, Y.L., Liou, D.L., Chen, Y.Z., Ge, N.J., Zhang, Z.Q., Sun, S.-S., Cong, B.L., Zhang, R.Y., Hart, S.R., Wang, S.S., 1993. Collision of the North China and Yangtse Blocks and formation of coesite-bearing eclogites: timing and processes. Chemical Geology 109, 89–111.

Li, S., Mooney, W.D., Fan, J., 2006. Crustal structure of mainland China from deep seismic sounding data. Tectonophysics 420, 239–252.

Liu, G., 1987. The Cenozoic rift system of North China Plain and the deep internal processes. Tectonophysics 133, 277–285.

Liu, D., Nutman, A.P., Compston, W., Wu, J., She, Q., 1992. Remnants of ≥3800 Ma crust in the Chinese part of the Sino-Korean craton. Geology 20, 339–342.

Liu, G.D., Hao, T.Y., Liu, Y.K., 1997. The macroscopically geotectonic framework of China and its relationship with mineral source: knowledge from the geophysical data. Chinese Science Bulletin 42, 113–118 (in Chinese).

Liu, H.F., Liang, H.S., Li, X.Q., Yin, J.G., Zhu, D.F., Liu, L.Q., 2000. The coupling mechanisms of Mesozoic–Cenozoic rift basins and extensional mountain system in eastern China. Earth Science of Geosciences 7, 477–486 (in Chinese).

Liu, M., Cui, X., Liu, F., 2004. Cenozoic rifting and volcanism in eastern China: a mantle dynamic link to the Indo–Asian collision? Tectonophysics 393, 29–42.

Ma, X.Y., 1989. Lithospheric Dynamics Map of China and Adjacent Seas (1:4,000,000) and Explanatory Notes. Geological Publishing House, Beijing, China.

Ma, X., Wu, D., 1987. Cenozoic extensional tectonics in China. Tectonophysics 133, 243–255.

Machetel, P., Humler, E., 2003. High temperature during Cretaceous avalanche. Earth and Planetary Science Letters 208, 125–133.

Maruyama, S., Isozaki, Y., Kimura, G., Terabayashi, M., 1997. Paleogeographic maps of the Japanese Islands: plate tectonic synthesis from 750 Ma to the present. Island Arc 6, 121–142.
Menzies, M.A., Xu, Y.G., 1998. Geodynamics of the North China Craton. In: Flower, M., Chung, S.L., Lo, C.H., Lee, T.Y. (Eds.), Mantle Dynamics and Plate Interactions in East Asia: American Geophysics Union Geodynamics Series, vol. 27, pp. 155–165.
Menzies, M.A., Fan, W.M., Zhang, M., 1993. Palaeozoic and Cenozoic lithoprobes and the loss of N120 km of Archaean lithosphere, Sino-Korean craton, China. In: Prichard, H.M., Alabaster, T., Harris, N.B.W., Neary, C.R. (Eds.), Magmatic Processes and Plate Tectonics: Geological Society Special Publication, vol. 76, pp. 71–78.
Miller, M.S., Kennett, B.L.N., 2006. Evolution of mantle structure beneath the northwest Pacific: evidence from seismic tomography and paleogeographic reconstructions. Tectonics 25, TC4002. doi:10.1029/2005TC001909.
Northrup, C.J., Royden, L.H., Burchfiel, B.C., 1995. Motion of the Pacific plate relative to Eurasia and its potential relation to Cenozoic extension along the eastern margin of Eurasia. Geology 23 (8), 719–722.
Ohtani, E., Litasov, K., Hosoya, T., Kubo, T., Kondo, T., 2004. Water transport into the deep mantle and formation of a hydrous transition zone. Physics of the Earth and Planetary Interiors 143, 255–269.
Omori, S., Komabayashi, T., Maruyama, S., 2004. Dehydration and earthquakes in the subducting slab: empirical link in intermediate and deep seismic zones. Physics of the Earth and Planetary Interiors 146, 297–311.
Owens, T.J., Nyblade, A.A., Gurrola, H., Langston, C.A., 2000. Mantle transition zone structure beneath Tanzania. Geophysical Research Letter 27, 827–830.
Pan, G.T., Mo, X.X., Hou, Z.Q., Zhu, D.C., Wang, L.Q., Li, G.M., Zhao, Z.D., Geng, Q.R., Liao, Z.L., 2006. Spatial–temporal framework of the Gangdese Orogenic Belt and its evolution. Acta Petrologica Sinica 22 (3), 521–533.
Pei, S., Zhao, J., Sun, Y., Xu, Z., Wang, S., Liu, H., et al., 2007. Upper mantle seismic velocities and anisotropy in China determined through Pn and Sn tomography. Journal of Geophysical Research 112, B05312. doi:10.1029/2006JB004409.
Petitjean, S., Rabinowicz, M., Grégoire, M., Chevrot, S., 2006. Differences between Archean and Proterozoic lithospheres: assessment of the possible major role of thermal conductivity. Geochemistry Geophysics Geosystems 7, Q03021. doi:10.1029/2005GC001053.
Ratschbacher, L., Hacker, B.R., Webb, L.E., McWilliams, M., Ireland, T., Dong, S.W., Calvert, A., Chateigner, D., Wenk, H.R., 2000. Exhumation of the ultrahigh-pressure continental crust in east central China: Cretaceous and Cenozoic unroofing and the Tan-Lu fault. Journal of Geophysical Research 105, 13,303–13,338.
Ren, J.S., 1990. Evolution of the Continental Lithospheric Texture and Mineralization in the East of China and Adjacent Areas. Scientific Publication House. (in Chinese).
Ren, J., Tamaki, K., Li, S., et al., 2002. Late Mesozoic and Cenozoic rifting and its dynamic setting in Eastern China and adjacent areas. Tectonophysics 344, 175–205.
Revenaugh, J., Jordan, T.H., 1991. Mantle layering from ScS reverberations: 2. The transition zone. Journal of Geophysical Research 96, 19,763–19,780.
Ringwood, A.E., 1991. Phase-transformations and their bearing on the constitution and dynamics of the mantle. Geochimica et Cosmochimica Acta 55 (8), 2083–2110.
Rudnick, R.L., Gao, S., Yuan, H.L., Puchtell, I., Walker, R., 2006. Persistence of Paleoproterozoic Lithospheric Mantle in the Central Zone of the North China Craton. Abstract for the International Conference on Continental Volcanism—IAVCEI.
Rychert, C.A., Fischer, K.M., Rondenay, S., 2005. A sharp lithosphere–asthenosphere boundary imaged beneath eastern North America. Nature 436, 542–545.
Savage, B., Silver, P.G., 2008. Evidence for a compositional boundary within the lithospheric mantle beneath the Kalahari craton from S receiver functions. Earth and Planetary Science Letters 272, 600–609.
Schutt, D.L., Dueker, K., Yuan, H., 2008. Crust and upper mantle velocity structure of the Yellowstone hot spot and surroundings. Journal of Geophysical Research 113, B03310. doi:10.1029/2007JB005109.
Sengör, A.M.C., Natal'in, B.A., Burtman, V.S., 1993. Evolution of the Altaid tectonic collage and Paleozoic crustal growth in Eurasia. Nature 364, 299–307.
Shomali, Z.H., Roberts, R.G., Pedersen, L.B., the TOR Working Group, 2006. Lithospheric structure of the Tornquist Zone resolved by nonlinear P and S teleseismic tomography along the TOR array. Tectonophysics 416, 133–149.
Smith, A.D., 2007. A plate model for Jurassic to recent intraplate volcanism in the Pacific ocean basin. In: Foulger, G.R., Jurdy, D.M. (Eds.), Plates, Plumes, and Planetary Processes. Geological Society of America, pp. 471–496.
Stuart, A.G., Keller, G.R., Luo, M., Goodell, P.C., 1991. Eastern Asia and the Western Pacific timing and spatial distribution of rifting in China. Tectonophysics 197, 225–243.
Sun, W., Ding, X., Hu, Y.H., Li, X.H., 2007. The golden transformation of the Cretaceous plate subduction in the west Pacific. Earth and Planetary Science Letters 262, 533–542.
Tan, Y., Helmberger, D.V., 2007. Trans-Pacific upper mantle shear velocity structure. Journal of Geophysical Research 104, B08301. doi:10.1029/2006JB004853.
Tang, Q., Chen, L., 2008. Structure of the crust and uppermost mantle of the Yanshan Belt and adjacent regions at the northeastern boundary of the North China Craton from Rayleigh wave dispersion analysis. Tectonophysics 455, 43–52.
Tang, Y.J., Zhang, H.F., Ying, J.F., 2006. Asthenosphere–lithospheric mantle interaction in an extensional regime: implication from the geochemistry of Cenozoic basalts from Taihang Mountains, North China Craton. Chemical Geology 233, 309–327.
Tian, Z., Han, P., Xu, K., 1992. The Mesozoic–Cenozoic East China rift system. Tectonophysics 208, 341–363.
Tommasi, A., Vauchez, A., 2001. Continental rifting parallel to ancient collisional belts: an effect of the mechanical anisotropy of the lithospheric mantle. Earth and Planetary Science Letters 185, 199–210.
Tommasi, A., Gibert, B., Seipold, U., Mainprice, D., 2001. Anisotropy of thermal diffusivity in the upper mantle. Nature 411, 783–786.
Vauchez, A., Barruol, G., Tommasi, A., 1997. Why do continents break up parallel to ancient orogenic belts? Terra Nova 9, 62–66.
Wang, J.Y., Huang, S.P., Chen, M.X., 1996. Terrestrial heat flux map (in Chinese). In: Yuan, X.C. (Ed.), Geophysical Atlas in China. Geophysical Publishing House, Beijing, p. 102.
Wang, Y.J., Fan, W.M., Zhang, H.F., Peng, T.P., 2006. Early Cretaceous gabbroic rocks from the Taihang Mountains: implications for a paleosubduction-related lithospheric mantle beneath the central North China Craton. Lithos 86, 281–302.
Wei, W., Ye, G., Jin, S., et al., 2008. Geoelectric structure of lithosphere beneath eastern North China: features of a thinned lithosphere from magnetotelluric soundings. Earth Science Frontiers 15, 204–216 (in Chinese with English abstract).
Wilde, S.A., Zhou, X.H., Nemchin, A.A., Sun, M., 2003. Mesozoic crust–mantle beneath the North China craton: a consequence of the dispersal of Gondwanaland and accretion of Asia. Geology 31, 817–820.
Wu, F.-Y., Walker, R.J., Ren, X.-W., Sun, D.-Y., Zhou, X.-H., 2003a. Osmium isotopic constraints on the age of lithospheric mantle beneath northeastern China. Chemical Geology 196, 107–129.
Wu, F.Y., Ge, W.C., Sun, D.Y., 2003b. Discussion on lithospheric thinning in eastern China. Earth Science Frontiers 10, 51–60 (in Chinese).
Wu, F.Y., Lin, J.Q., Simon, A.W., Zhang, X.O., Yang, J.H., 2005. Nature and significance of the Early Cretaceous giant igneous event in eastern China. Earth and Planetary Science Letters 233, 103–119.
Wu, F.Y., Xu, Y.G., Gao, S., Zheng, J.P., 2008. Controversial on studies of the lithospheric thinning and craton destruction of North China. Acta Petrologica Sinica 24, 1145–1174 (in Chinese with English abstract).
Xiao, W.J., Windley, B.F., Hao, J., Li, J.L., 2002. Arc-ophiolite obduction in the Western Kunlun Range (China): implications for the Palaeozoic evolution of central Asia. Journal of the Geological Society, London 159, 517–528.
Xiao, W.J., Windley, B.F., Hao, J., Zhai, M., 2003. Accretion leading to collision and the Permian Solonker suture, Inner Mongolia, China: termination of the central Asian orogenic belt. Tectonics 22, 1069. doi:10.1029/2002TC001484.
Xiao, W.J., Windley, B.F., Yong, Y., et al., 2009. Early Paleozoic to Devonian multiple-accretionary model for the Qilian Shan, NW China. Journal of Asian Earth Sciences 35, 323–333.
Xu, Y.G., 2001. Thermotectonic destruction of the Archean lithospheric keel beneath eastern China: evidence, timing, and mechanism. Physics and Chemistry of the Earth A 26, 747–757.
Xu, Y.G., 2007. Diachronous lithospheric thinning of the North China Craton and formation of the Daxin'anling–Taihangshan gravity lineament. Lithos 96, 281–298.
Xu, P., Zhao, D., 2009. Upper-mantle velocity structure beneath the North China Craton: implications for lithospheric thinning. Geophysical Journal International 177, 1279–1283.
Xu, Y.G., Chung, S.L., Ma, J.L., Shi, L.B., 2004a. Contrasting Cenozoic lithospheric evolution and architecture in the eastern and western Sino-Korean craton: constraints from geochemistry of basalts and mantle xenoliths. Journal of Geology 112, 593–605.
Xu, Y.G., Huang, X.L., Ma, J.L., Wang, Y.B., Iizuka, Y., Xu, J.F., Wang, Q., Wu, X.Y., 2004b. Crustal–mantle interaction during the thermo-tectonic reactivation of the North China Craton: SHRIMP zircon U–Pb age, petrology and geochemistry of Mesozoic plutons in western Shandong. Contributions to Mineralogy and Petrology 147, 750–767.
Yang, J.H., Wu, F.Y., Wilde, S.A., 2003. Geodynamic setting of large-scale Late Mesozoic gold mineralization in the North China Craton: an association with lithospheric thinning. Ore Geology Reviews 23, 125–152.
Ye, H., Zhang, B., Mao, F., 1987. The Cenozoic tectonic evolution of the Great North China: two types of rifting and crustal necking in the Great North China and their tectonic implications. Tectonophysics 133, 217–227.
Yin, A., 2000. Mode of Cenozoic east–west extension in Tibet suggesting a common origin of rifts in Asia during the Indo-Asian collision. Journal of Geophysical Research 105, 21,745–21,759.
Yin, A., Nie, S.Y., 1993. An indentation model for the North and South China collision and the development of the Tan-Lu and Honam Fault Systems, eastern Asia. Tectonics 12, 801–813.
Yin, A., Nie, S.Y., 1996. A Phanerozoic palinspastic reconstruction of China and its neighboring regions. In: Yin, A., Harrison, M. (Eds.), The Tectonic Evolution of Asia. Cambridge University Press, pp. 442–484.
Zhai, M.G., Liu, W.J., 2003. Paleoproterozoic tectonic history of the North China craton: a review. Precambrian Research 122, 183–199.
Zhai, M.G., Zhu, R.X., Liu, J.M., et al., 2004. Time range of Mesozoic tectonic regime inversion in eastern North China Block. Science in China, Series D Earth Sciences 47 (2), 151–159.
Zhang, K.J., 1997. North and South China collision along the eastern and southern North China margins. Tectonophysics 270, 145–156.
Zhang, H.F., 2005. Transformation of lithospheric mantle through peridotite-melt reaction: a case of Sino-Korean craton. Earth and Planetary Science Letters 237, 768–780.
Zhang, H.F., 2007. Temporal and spatial distribution of Mesozoic mafic magmatism in the North China Craton and implications for secular lithospheric evolution. Geological Society, London, Special Publications 280, 35–54.
Zhang, Y.-S., Tanimoto, M., 1993. High-resolution global upper mantle structure and plate tectonics. Journal of Geophysical Research 98, 9793–9823.
Zhang, Y.Q., Mercier, J.L., Vergély, P., 1998. Extension in the graben systems around the Ordos (China), and its contribution to the extrusion tectonics of south China with respect to Gobi-Mongolia. Tectonophysics 285, 41–75.
Zhang, H.F., Sun, M., Zhou, X.H., Fan, W.M., Zhai, M.G., Ying, J.F., 2002. Mesozoic lithosphere destruction beneath the North China Craton: evidence from major, trace element, and Sr–Nd–Pb isotope studies of Fangcheng basalts. Contributions to Mineralogy and Petrology 144, 241–253.
Zhang, Y.Q., Ma, Y.S., Yang, N., Shi, W., Dong, S., 2003. Cenozoic extensional stress evolution in North China. Journal of Geodynamics 36, 591–613.

Zhang, S.-H., Zhao, Y., Song, B., Yang, Z.-Y., Hu, J.-M., Wu, H., 2007. Carboniferous granitic plutons from the northern margin of the North China block: implications for a late Palaeozoic active continental margin. Journal of the Geological Society, London 164, 451–463.

Zhao, L., Zheng, T., 2005. Using shear wave splitting measurements to investigate the upper mantle anisotropy beneath the North China Craton: distinct variation from east to west. Geophysical Research Letter 32, L10309. doi:10.1029/2005GL0022585.

Zhao, L., Zheng, T., 2007. Complex upper-mantle deformation beneath the North China Craton: implications for lithospheric thinning. Geophysical Journal International 170, 1095–1099.

Zhao, G.C., Wilde, S.A., Cawood, P.A., Sun, M., 2001. Archean blocks and their boundaries in the North China Craton: lithological, geochemical, structural and *P–T* path constraints and tectonic evolution. Precambrian Research 107, 45–73.

Zhao, G.C., Sun, M., Wilde, S.A., 2003. Major tectonic units of the North China Craton and their Paleoproterozoic assembly. Science in China 46, 23–38.

Zhao, G.C., Sun, M., Wilde, S.A., Li, S.Z., 2005. Late Archean to Paleoproterozoic evolution of the North China Craton: key issues revisited. Precambrian Research 136, 177–202.

Zhao, D., Maruyama, S., Omori, S., 2007a. Mantle dynamics of Western Pacific and East Asia: insight from seismic tomography and mineral physics. Gondwana Research 11, 120–131.

Zhao, L., Zheng, T., Chen, L., Tang, Q., 2007b. Shear wave splitting in eastern China, implications for upper mantle deformation beneath continental margin. Physics of the Earth and Planetary Interiors 162, 73–84.

Zhao, L., Zheng, T., Lü, G., 2008. Insight into craton evolution: Constraints from shear wave splitting in the North China Craton. Physics of the Earth and Planetary Interiors 168, 153–162.

Zheng, J., O'Reilly, S.Y., Griffin, W.L., Lu, F., Zhang, M., 1998. Nature and evolution of Cenozoic lithospheric mantle beneath Shandong peninsula, Sino–Korean craton. International Geology Review 40, 471–499.

Zheng, J., O'Reilly, S.Y., Griffin, W.L., Lu, F., Zhang, M., Pearson, N.J., 2001. Relict refractory mantle beneath the eastern North China block: significance for lithosphere evolution. Lithos 57, 43–66.

Zheng, T., Chen, L., Zhao, L., Xu, W.W., Zhu, R., 2006. Crust–mantle structure difference across the gravity gradient zone in North China Craton: Seismic image of the thinned continental crust. Physics of the Earth and Planetary Interiors 159, 43–58.

Zheng, T., Chen, L., Zhao, L., Zhu, R., 2007. Crustal structure across the Yanshan belt at the northern margin of the North China Craton. Physics of the Earth and Planetary Interiors 161, 36–49.

Zheng, T., Zhao, L., Xu, W., Zhu, R., 2008a. Insight into the geodynamics of cratonic reactivation from seismic analysis of the crust–mantle boundary. Geophysical Research Letter 35, L08303. doi:10.1029/2008GL033439.

Zheng, T., Zhao, L., Xu, W., Zhu, R., 2008b. Insight into modification of North China Craton from seismological study in the Shandong Province. Geophysical Research Letter 35, L22305. doi:10.1029/2008GL035661.

Zheng, T., Zhao, L., Zhu, R.X., 2009. New evidence from seismic imaging for subduction during assembly of the North China Craton. Geology 37, 395–398.

Zhu, J., Cao, J., Cai, X., Yan, Z., Cao, X., 2002. High resolution surface wave tomography in east Asia and west Pacific marginal seas. Chinese Journal of Geophysics 45 (5), 646–664 (in Chinese with English abstract).

Zhu, R.X., Zheng, T., 2009. Destruction geodynamics and Paleoproterozoic plate tectonics of the North China Craton. Chinese Science Bulletin 54 (19), 3354–3366.